BIOLOGICAL MEMBRANES: THE PHYSICAL BASIS OF ION AND NONELECTROLYTE SELECTIVITY[1]

By Jared M. Diamond and Ernest M. Wright
Department of Physiology, University of California Medical Center
Los Angeles, California

Contents

[1] The survey of literature for this review was concluded in August 1968.

Basic to the function of cell membranes is the ability to select between closely similar ions and molecules, such as potassium and sodium, calcium and magnesium, alcohols and aldehydes, and esters and acids. An understanding of the principles underlying selectivity is relevant to the study of neurophysiology, active transport, passive permeation, enzyme activation, and membrane structure. The present chapter has a twofold purpose: to summarize experimental evidence concerning the distinctive and consistent selectivity patterns exhibited by biological membranes; and to review recent developments that have made it possible to account in large part for the main features of these patterns in terms of intermolecular and interatomic forces. Analyses of selectivity must begin by trying to explain as many phenomena as possible in terms of elementary physical concepts such as free energy, and in terms of the simplest principles governing the interactions of ions, such as Coulomb's law, or the simplest principles governing the interactions of nonelectrolytes, such as hydrogen bonding and van der Waals forces. While consideration of additional forces may prove necessary to interpret some more complex phenomena, explanations that do not take account even of the simplest forces cannot provide an adequate starting-point. The first half of this chapter is devoted to ion selectivity, while the second half deals with nonelectrolyte selectivity.

PART I. ION SELECTIVITY

Introduction

Potassium and sodium exhibit marked quantitative differences in their abilities to penetrate cell membranes at rest and during excitation, in their affinities for active transport mechanisms, and in their potency in activating enzymes. For example, resting nerve membrane is about 30 times more permeable to K^+ than to Na^+, while active nerve membrane is 10 times more permeable to Na^+ than to K^+. These differences form the basis for much of neurophysiology and for the maintenance of cell volume. However, K^+ and Na^+ are quite similar in their physical and chemical properties to each other and to the three other alkali cations in group I of the periodic table, lithium (Li^+), cesium (Cs^+), and rubidium (Rb^+). As far as their interactions with water and with simple anions are concerned, the five alkali cations can be well approximated as rigid, nonpolarizable, monopolar spheres differing only in radius. The mechanism of alkali-cation discrimination is therefore not only one of the central problems of cell physiology but also a question of basic physical interest. Analogous problems of biological importance and of equal physical interest are posed by discrimination among the alkaline-earth cations (Ca^{++}, Mg^{++}, Sr^{++}, Ba^{++}) and among the halide anions (Cl^-, Br^-, I^-, F^-).

Nonbiological systems, such as soils, minerals, ion exchange resins, and glass electrodes, also discriminate among the alkali cations and among ions of other groups. The ranges of selectivity patterns observed (the so-called "transition sequences" discussed below) show such striking and detailed similarities in nonbiological and in biological systems as to make it likely

that the underlying physical mechanism of discrimination is the same in both cases. As a result of theoretical studies stemming from Jenny in the late 1920s, further advanced by Bungenberg de Jong, recently stimulated by the development of the ion-specific glass electrodes and by accumulated measurements of biological sequences, but most of all as a result of the work of Eisenman (1–3), physical chemists interested in ion selectivity are now in general agreement concerning the theoretical framework for interpretation (see 4–6 for discussions).

We shall therefore begin by summarizing the alkali-cation selectivity patterns observed in nonliving systems and by tabulating recently determined patterns in biological systems for comparison. The basic physical principles governing alkali-cation equilibrium selectivity are then discussed in broad outline. The patterns and the physical basis of halide anion selectivity and of divalent-cation selectivity are similarly summarized. Finally, some physical determinants of ion selectivity, and some common misconceptions in the physiological literature, are re-examined in more detail.

Alkali-Cation Selectivity in Nonliving Systems

Historically, the problem of alkali-cation selectivity in nonliving systems first received systematic attention in studies conducted by geologists and chemists early in this century on ion exchange by soils. The ability of soils to bind different alkali cations with different strengths was found to be due to the presence of naturally occurring aluminosilicate minerals which were isolated, studied as ion exchangers, and compared with artificial aluminosilicates. For example, Jaeger (7) found that the mineral ultramarine at 160° C bound Li^+ the most strongly of the five alkali cations and Cs^+ the least strongly, the whole sequence being $Li^+ > Na^+ > K^+ > Rb^+ > Cs^+$. The measured ionic (nonhydrated) radii of the alkali cations increase in this order, Li^+ being smallest and Cs^+ largest [Li^+ 0.60Å, Na^+ 0.95Å, K^+ 1.33Å, Rb^+ 1.48Å, Cs^+ 1.69Å, from Pauling (8)]. It was therefore natural to interpret the ion exchange selectivity of ultramarine in terms of the closeness with which nonhydrated positive ions of different sizes could approach the negatively charged aluminosilicate site:[2] the center of charge of the small Li^+ would be closest to the negative site, Li^+ would experience the greatest electrostatic attractive force, and would therefore be the most strongly bound.

On the other hand, many other aluminosilicates, such as a permutit studied by Jenny (9), exhibited the reverse sequence of binding strength, $Cs^+ > Rb^+ > K^+ > Na^+ > Li^+$. In aqueous solution the measured mobilities

[2] In the language of ion exchange a site is defined as a group fixed in the membrane and bearing a net ionic charge (e.g., $AlOSi^-$, COO^-, etc.) which is balanced electrically by oppositely charged mobile ions. In this chapter we shall also use the word site loosely (e.g., in the expression, ion:site interactions) to mean whatever membrane group is the nearest neighbor of a mobile permeating ion, whether the membrane group bears a net charge or not (see p. 607 and footnote 3, p. 592, for discussion).

decrease, and hence the calculated Stokes-law hydrated radii increase, in the same order (the so-called lyotropic series): Li^+ has the smallest ionic radius but also the smallest free-solution mobility and thus the largest apparent hydrated size. The reason is that the smaller the ion, the nearer to water molecules its center of charge lies, and hence the more strongly it is hydrated. Jenny therefore postulated that the different selectivity patterns of ultramarine and of permutit arose because the ions were present in the nonhydrated form in the former case, in the hydrated form in the latter case; and that Cs^+ was most strongly bound in permutit because it had the smallest hydrated size and could now approach closest to the negative charge of the aluminosilicate site.

Unfortunately for this simple interpretation, it soon became apparent that still other selectivity patterns than these two were exhibited by some other minerals. For example, Barrer, Rees & Ward (10) found that a synthetic aluminosilicate called Linde A, which belongs to the class of aluminosilicates called zeolites, binds alkali cations in the sequence $Na^+ > K^+ > Rb^+ > Li^+ > Cs^+$. The patterns $Cs^+ > K^+ > Rb^+ > Na^+ > Li^+$, $K^+ > Cs^+ > Rb^+ > Na^+ > Li^+$, $Na^+ > K^+ > Rb^+ > Cs^+ > Li^+$, $Na^+ > K^+ > Li^+ > Rb^+ > Cs^+$, or $Na^+ > Li^+ > K^+ > Rb^+ > Cs^+$ were found in other zeolites. These puzzling patterns corresponded neither to the order of the nonhydrated radii nor to the order of the apparent hydrated radii, and Jenny (9, p. 2252) referred to them as "irregularities in the lyotropic series".

A second class of objects besides soil minerals marked by "irregularities" in alkali-cation selectivity was provided by the development of the commercial ion exchange resins (4). Most of these consisted of a polystyrene matrix crosslinked to varying extents with divinylbenzene and bearing negatively charged groups, such as sulfonate or carboxyl, which acted as sites for exchange of cations. In some resins the alkali cations were bound in the order of their apparent hydrated radii (the lyotropic series), as in Jenny's permutit. However, sequences other than the lyotropic series or the sequence of the ionic radii were also obtained. For instance, Reichenberg (4) found that the affinity sequence for a resin with sulfonate groups and with moderate crosslinking (10–15 per cent divinylbenzene) was $K^+ > Cs^+ > Na^+ > Li^+$ (Rb^+ not tested), which differs from the lyotropic series in that the order of K^+ and Cs^+ is reversed.

A third source of "irregularities" came from electrical measurements on permselective collodion membranes, which are permeable to cations but not to anions by virtue of containing negatively charged carboxyl groups. Ling & Kushnir (see 1) estimated the relative permeabilities of different alkali cations from the electrical potential difference developed when the membrane separated solutions of two different alkali cations. Depending upon how the membranes were prepared, the relative permeabilities were in one of three sequences: $Cs^+ > Rb^+ > K^+ > Na^+ > Li^+$, $Cs^+ > K^+ > Rb^+ > Na^+ > Li^+$, or $K^+ > Cs^+ > Rb^+ > Na^+ > Li^+$. The first of these is the lyotropic series, but the other two sequences are neither in the order of nonhydrated size nor of apparent hydrated size.

At this point one might wonder whether systematic study would show the number of alkali-cation selectivity sequences to be so large as to be essentially random and chaotic and to defy generalization, since permutation of the five alkali cations (5!) would yield 120 possible selectivity sequences. However, certain sequences were found repeatedly in these studies of minerals, resins, and collodion membranes, while other permutations were never observed. For instance, systems preferring Na^+ to Cs^+ generally preferred K^+ to Rb^+ and Rb^+ to Cs^+, though they might or might not prefer Na^+ to K^+, while systems preferring Li^+ to Na^+ generally did prefer Na^+ to K^+.

The systematic search for regularities in cation selectivity sequences was greatly facilitated by the development of the cation-selective glass electrodes. Glass electrodes which were made of SiO_2 and the oxide of an alkali metal and whose electrical potential differences were governed almost solely by the hydrogen ion (activity) gradient had been known since the time of Cremer (1906). Hughes (11) and others showed that these pH electrodes exhibited an "alkaline error", i.e., a sensitivity to alkali metal ions as well as to $[H^+]$, which introduced an error into pH determinations at high pH (low H^+ concentration) and whose magnitude was correlated with the amounts of Al_2O_3 or B_2O_3 present in the glass. In 1957 Eisenman, Rudin & Casby (12) exploited this finding by preparing three-component glasses of $SiO_2+Al_2O_3+Na_2O$ mixed in varying proportions and found that varying the glass composition produced systematic variations in selectivity among the alkali cations and other ions; they thereby obtained practical electrodes responding preferentially to different alkali cations. In addition to the SiO_2-Al_2O_3-Na_2O glasses, these authors also studied glasses in which Na_2O had been replaced by Li_2O or K_2O, Al^{+++} had been replaced by B^{+++} or Sc^{+++}, and SiO_2 had been replaced by GeO_2. Later the effects of numerous other components added to SiO_2 plus the alkali oxide were tested (13). The particular alkali cation to which a given glass was most sensitive did not need to be a component of the glass. The selectivity preferences of most of these glasses for the five alkali cations fell into one of 11 sequences, the other 109 possible permutations not being observed in practice. The selectivities of most soil minerals and synthetic aluminosilicate ion exchangers, resins, and collodion membranes were noted in retrospect to belong to the same 11 sequences (1). They are:

I	$Cs^+ > Rb^+ > K^+ > Na^+ > Li^+$
II	$Rb^+ > Cs^+ > K^+ > Na^+ > Li^+$
III	$Rb^+ > K^+ > Cs^+ > Na^+ > Li^+$
IV	$K^+ > Rb^+ > Cs^+ > Na^+ > Li^+$
V	$K^+ > Rb^+ > Na^+ > Cs^+ > Li^+$
VI	$K^+ > Na^+ > Rb^+ > Cs^+ > Li^+$
VII	$Na^+ > K^+ > Rb^+ > Cs^+ > Li^+$
VIII	$Na^+ > K^+ > Rb^+ > Li^+ > Cs^+$
IX	$Na^+ > K^+ > Li^+ > Rb^+ > Cs^+$
X	$Na^+ > Li^+ > K^+ > Rb^+ > Cs^+$
XI	$Li^+ > Na^+ > K^+ > Rb^+ > Cs^+$

Each sequence differs from the preceding and following sequence only in inversion of the positions of one pair of cations; the sequences II through X constitute "transition sequences" linking sequence I, the lyotropic series defined by increasing apparent hydrated size, to sequence XI, defined by increasing nonhydrated size. That this sequential arrangement of the transition series corresponds to some underlying reality is shown by the fact that as one increases the Al_2O_3/Na_2O ratio in the electrode glass, or raises the pH from an acid value, one proceeds through the sequences in the direction I through XI. Beginning with sequence I, the first inversions encountered (sequences I–IV) involve Cs^+, Rb^+, and K^+, the three largest and hence least strongly hydrated cations; then (sequences IV–VII) the position of Na^+, which is more strongly hydrated, inverts with respect to each of these three cations in turn; and finally (sequences VII–XI) Li^+, the smallest and most strongly hydrated cation, inverts with respect to the other four to yield sequence XI, in which affinity decreases with increasing nonhydrated size. The underlying reason why the inversions start with the largest and end with the smallest ion is discussed on p. 606.

In addition to the regular qualitative pattern defined by these 11 sequences actually observed out of 120 possible permutations, quantitative regularities were also observed in the magnitudes of selectivity encountered in glass electrodes, aluminosilicate ion exchangers, and collodion membranes: a given sequence also implied a given range of selectivity ratios. For instance, sequence IX ($Na^+ > K^+ > Li^+ > Rb^+ > Cs^+$) implied approximately the ranges of selectivity ratios $Na^+/K^+ = 5$ to 80, $Li^+/K^+ = 0.2$ to 1, $Rb^+/K^+ = 0.1$ to 0.2, $Cs^+/K^+ = 0.006$ to 0.01. The existence of these quantitative patterns became clear in the course of attempts to find glass electrodes with higher or differing selectivities by varying glass components or their proportions: such attempts only yielded more electrodes with the same range of selectivity magnitudes (1, 13). When the selectivity ratios for many systems are plotted on the same graph as a function of, say, the Na^+/K^+ selectivity ratio, one obtains a set of five intersecting curves (the so-called selectivity isotherms) for the five alkali cations, the intersections determining transitions from one sequence to the next. In the vicinity of sequence II the Cs^+, Rb^+, and K^+ isotherms lie close to each other, and the exact sequence of intersections varies somewhat among different systems, so that $Cs^+ > K^+ > Rb^+ > Na^+ > Li^+$ (sequence IIa) and $K^+ > Cs^+ > Rb^+ > Na^+ > Li^+$ (sequence IIIa) are obtained in some systems as minor quantitative variants of sequences II and III. Since these selectivity isotherms for the alkali cations have been published previously [e.g., Figure 8 of (1), Figure 8 of (2), Figure 7 of (3)], they are not reproduced here but are similar in principle to the halide isotherms and alkaline-earth isotherms derived in Figures 1 and 2 of this chapter. Detailed discussion of selectivity isotherms and their construction will therefore be postponed until we consider Figures 1 and 2; the meaning of the present paragraph should then become clearer.

Alkali-Cation Selectivity in Biological Systems

Relative potencies of the alkali cations have been determined by varied methods for many different kinds of effects in a wide variety of biological systems. These effects include: the ability to mimic potassium in controlling the resting potential of cell membranes; the ability to mimic sodium in controlling the height of the action potential in nerve, muscle, and other excitable tissues; contributions to membrane conductance; passive one-way tracer fluxes across membranes; affinities for active transport mechanisms; ability to activate Na^+- or K^+-requiring enzymes; the permeability induced in thin lipid membranes by peptide and polyene antibiotics such as valinomycin; and miscellaneous effects such as stimulation of respiration in yeast and stimulation of the salt receptor in blowflies.

This large and diverse body of experimental results may be briefly summarized by saying that the alkali-cation selectivity patterns determined in most biological systems belong to the same 11 selectivity patterns (and are characterized by similar ranges of selectivity and permeability ratios) as those found in nonliving systems. Since earlier evidence for these statements has been reviewed in detail elsewhere (3, 14), we shall mention only some of the more recent studies of selectivity patterns:

Berridge (15) found that the rate of urine flow in Malpighian tubules of the blowfly *Calliphora erythrocephala* was stimulated in the order $K^+ > Rb^+ > Cs^+ > Na^+ > Li^+$ (sequence IV).

The permeability sequence in rabbit gallbladder epithelium was determined by Wright & Diamond (16) as $K^+ > Na^+ > Cs^+$ (sequence V or VI) at pH 7, and as $K^+ > Cs^+ > Na^+$ (sequence III or IV) at pH 2.4.

The potency order for replacing Na^+ in the "sodium channel" of squid axon was given by Chandler & Meves (17) as $Li^+ > Na^+ > K^+ > Rb^+ > Cs^+$ (sequence XI), extending the familiar observation that Li^+ can replace Na^+ in generating spikes but that the action potential selects sodium over potassium.

Salt receptors of blowflies (18) are stimulated in the order $K^+ > Na^+ > Rb^+ > Cs^+ > Li^+$ (sequence VI).

Much recent interest has been attracted by the selective cation permeability induced in thin lipid membranes by small quantities of large-ring compounds, such as the cyclic polypeptide antibiotics related to valinomycin, the macrolide actins, the carboxyl antibiotics related to nigericin, and the cyclic "crown" polyethers. Selectivity patterns determined by Pressman (19) for six of these compounds, based on cation migration from an aqueous phase to a butanol-toluene phase containing the antibiotic, are: nigericin, $K^+ > Rb^+ > Na^+ > Cs^+ > Li^+$ (sequence V); dianemycin, $Na^+ > K^+ > Rb^+$, $Cs^+ > Li^+$ (sequence VII); X-206, $K^+ > Rb^+ > Na^+ > Cs^+ > Li^+$ (sequence V); X-537, $Cs^+ > K^+ > Rb^+ > Na^+ > Li^+$ (sequence IIa); valinomycin, $Rb^+ > K^+ > Cs^+ > Na^+ > Li^+$ (sequence III); monensin, $Na^+ > K^+ > Rb^+ > Cs^+$ (se-

quence VII or higher). $Rb^+ > K^+ > Cs^+ > Na^+ > Li^+$ (sequence III) was obtained by Mueller & Rudin (20) for thin lipid membranes containing valinomycin, enniatin B, gramicidin A, or dinactin, by Lev & Buzhinsky (21) for thin lipid membranes containing valinomycin, and by Andreoli, Tieffenberg & Tosteson (22) for thin membranes made from sheep erythrocyte lipids after addition of valinomycin. Eisenman, Ciani & Szabo (23) found $K^+ > Rb^+ > Cs^+ > Na^+ > Li^+$ (sequence IV) for permeabilities of lipid bilayers containing monactin or the cyclic polyether XXXI [names of these ethers follow Pedersen's (24) terminology], for the conductance of bilayers containing monactin, for cation migration from an aqueous phase into a hexane or methylene chloride phase containing monactin, and for migration into a methylene chloride phase containing the polyether XXXI; $Cs^+ > Rb^+ > K^+ > Na^+ \sim Li^+$ (sequence I) for the conductance of bilayers containing polyether XXXI; and $K^+ > Rb^+ > Na^+ > Cs^+ > Li^+$ (sequence V) for migration into a hexane phase containing polyether XXXI. Studying migration into a methylene chloride phase containing a polyether, Pedersen (25) obtained sequence IV for polyethers V′, VI′, and X′; sequence VII for polyether IV′; and sequence XI for polyether II′.

Effectiveness in maintaining the potential difference across the isolated beef cornea (26) (presumably reflecting affinities for an active transport mechanism) is in the order $Li^+ > Na^+ > K^+, Rb^+$ (sequence XI).

The enzyme microsomal phosphatase from gastric mucosa (27) is stimulated in the order $K^+ > Rb^+ > Cs^+ > Na^+, Li^+$ (sequence IV).

From changes in electrophoretic velocity Bungenberg de Jong (28) estimated binding affinities to the colloids pectinate, pectate, and agar to decrease in the order $Cs^+ > Rb^+ > K^+ > Na^+ > Li^+$ (sequence I).

DNA from calf thymus and RNA from yeast (29) bind cations in the order $Li^+ > Na^+ > K^+ > Rb^+ > Cs^+$ (sequence XI).

Relative affinities for the cation transport system in yeast (30) are $K^+ > Rb^+ > Cs^+ > Na^+ > Li^+$ (sequence IV).

The order of equilibrium distribution ratios for muscle cells (31) is $K^+ > Rb^+ > Cs^+ > Na^+$ (sequence IV).

Myosin ATPase (32) is inhibited by alkali cations in the order $Li^+ > Na^+ > K^+ > Rb^+ > Cs^+$ (sequence XI).

The sequence for stimulation of sodium extrusion in squid axons was determined as $K^+ > Rb^+ > Cs^+$ (sequence IV or higher) by Sjodin & Beaugé (33) from efflux rate constants of radioactive sodium. Baker & Connelly (34) obtained the same sequence by a different method, measurement of oxygen consumption, for stimulation of sodium extrusion in crab nerve.

As deduced by Lindley & Hoshiko (35) from measurements of changes in the potential difference across frog skin, the permeability order is $Na^+ > Li > Rb^+, K^+, Cs^+$ (approximately sequence X) at the outer surface of the skin, but $K^+ > Rb^+ > Cs^+ > Li^+ > Na^+$ (differs from sequence IV only in the higher potency of Li^+) at the inner surface.

Maizels (36) found that the effect on Na^+ efflux from red cells of a second

alkali cation, present in the bathing solution and inside the cells, depended upon the sodium concentration: $K^+ > Cs^+ > Rb^+ > Li^+$ (sequence IIIa) at high $[Na^+]$, $Cs^+ > K^+ > Rb^+ > Li^+$ (sequence IIa) at lower $[Na^+]$, and $Cs^+ > K^+ > Li^+ > Rb^+$ and $Cs^+ > Li > K^+ > Rb^+$ (deviant sequences due to anomalous position of Li^+) at still lower $[Na^+]$.

There are three other instances similar to the last two sequences reported by Maizels and the pattern for frog skin inner surface, which differ from the usual patterns in that transitions involving the smallest cation Li^+ apparently occur before rather than after other transitions.

Actomyosin ATPase is inhibited by alkali cations (37) in the order $Cs^+ > Li^+ > Rb^+$, $K^+ > Na^+$ (differs from sequence I in Li^+ inversions but no other inversions).

Relative effects on electrophoretic velocities of phosphate colloids are $Li^+ > Cs^+ > Rb^+ > Na^+ > K^+$ for egg lecithin and $Li^+ > Cs^+ > Na^+ > Rb^+ > K^+$ for the alcohol-soluble fraction of soya bean phosphatide (28). These two colloid cases reverse completely the usual order of transitions, in that Li^+ inversions are being followed by inversions for the next smallest cation Na^+, which must in turn be followed by inversions among the three largest cations Cs^+, Rb^+, and K^+.

Selectivity isotherms may be constructed from these biological data as already mentioned in connection with the data from nonliving systems (p. 586) and as will be explained in more detail when we come to the halide and alkaline-earth isotherms (Figures 1 and 2 of this chapter). The resulting biological isotherms and the glass electrode isotherms differ principally in a shift in the Li^+ curve, such that biological systems discriminate against Li^+ less sharply than do glasses even when Li^+ stands qualitatively in one of the usual "glass" sequences, as is generally the case. This point may be appreciated by comparing Figure 9 of (3) with the upper half of Figure 7 of the same reference. The significance of this quantitative Li^+ shift and of the more marked sequence anomalies just cited involving Li^+ is discussed on p. 607. A further feature of both the biological and the glass isotherms to be discussed later is the indication provided by a few systems that the Rb^+ and Cs^+ isotherms re-intersect the other isotherms after sequence XI to commence a new set of sequences. This is illustrated by one recent example: the sequence $Li^+ > Na^+ > Rb^+ > K^+ > Cs^+$ for affinities to DNA (38), differing from sequence XI in the Rb^+-K^+ reversal.

The Origin of Alkali-Cation Equilibrium Selectivity

Early attempts to explain the origin of alkali-cation equilibrium selectivity and to predict the observed transition sequences were put forward by Jenny (9, 39) in 1927, by Bungenberg de Jong (28, 40) in 1939, by Gregor (41) in 1948, and by Ling (42) in 1952. Jenny (9, p. 2252 and p. 2257) reasoned: "The observed irregularities [i.e., the transition sequences] in the lyotropic series of natural aluminum silicates can be interpreted as various stages in the reversal of the normal hydration order of the exchanging cat-

ions. . . . Obviously the most hydrated ion will be first affected by dehydration processes. . . . It appears that these 'hydrodynamic radii' [=hydrated ion radii] vary accordingly to the nature of the colloidal system." Jenny did not discuss what factors might be responsible for this progessive dehydration of ions. His assumption that the most hydrated ion should be first to become dehydrated leads to the prediction that inversions involving Li^+ should occur first, those involving Na^+ next, and those involving K^+, Rb^+, and Cs^+ last as one proceeds from sequence I to XI, whereas the actual order in most cases is the opposite of this prediction, as already discussed (p. 586).

Bungenberg de Jong (40; 28, pp. 287–88) attributed selectivity to the relative polarizabilities of the negatively charged ion exchange site and of water. Polarization either of the site or of water by a cation would increase site:cation or water:cation electrostatic attraction and would be stronger for smaller cations. A site much more polarizable than water would yield sequence XI, the order of nonhydrated radii; a site much less polarizable than water would yield sequence I, the order of apparent hydrated size; and intermediate degrees of polarizability would yield transition sequences. However, the predicted transition sequences are the reverse of most of those actually observed, since Bungenberg de Jong's postulate predicts, as did Jenny's, that reversals involving Li^+ should occur first as one proceeds from sequence I to XI. Gregor (41) related the ion exchange equilibrium constant to the different hydrated volumes of different cations, the elastic counterpressure built up within the exchanger, and the stripping of water molecules from hydrated ions. His theory was criticized for its failure to explain the apparent differential stripping of hydration water that had to be postulated to account for transitions, and for the arbitrariness inherent in using apparent hydrated sizes as the reference point. Ling (42) calculated electrostatic forces between hydrated cations and anionic sites, but was unable (43) to account on this basis for sequences inverted from those of apparent hydrated sizes, such as $Na^+ > K^+$, and was also criticized, as was Gregor, for using apparent hydrated sizes as his reference point. Thus, these earlier theories of ion selectivity all broke down over their failure to solve the problem of the transition sequences.

The interpretation of alkali-cation equilibrium selectivity which is now generally accepted by physical chemists (4–6), and which correctly predicts the transition sequences, was put forward by Eisenman (1–3, 13, 14) in 1961. Eisenman's theory attributes selectivity to the different attractive forces, mainly Coulombic, exerted on different cations by water on the one hand and by membrane negative charges on the other. Before discussing in detail how the strength

let us consider first some simple observations indicating that such is actually the case, from glass electrode studies and from a recent study on a biological membrane.

The glass electrodes specific for alkali cations are ion exchangers in which the negatively charged site for cation exchange is $(AlOSi)^-$. Protons can

screen the negative charge on the site, reducing the effective negative charge strength experienced by a positive counterion. It is found experimentally [cf. Figure 3 of (1)] that the selectivity pattern of a given glass electrode shows some pH dependence, shifting in the direction from sequence XI (order of nonhydrated size) towards sequence I (order of free-solution mobilities) with decreasing pH (increasing H^+ concentration). For example, a glass with the composition 18.3 per cent Na_2O–7.1 per cent Al_2O_3–74.6 per cent SiO_2 exhibits selectivity sequence IX above pH 7, sequence VIII between pH 7 and 5, sequence VII between pH 5 and 3.5, and sequences VI, V, IV, and III in turn as one goes from pH 3.5 to pH 2. A second way of screening the negative $(AlOSi)^-$ sites in a Na_2O–Al_2O_3–SiO_2 electrode is with the Na^+ of the glass itself, by increasing the proportion of Na_2O to Al_2O_3 in the glass. An increased Na^+/Al^{+++} ratio of the glass shifts selectivity in the direction from sequence XI to sequence I (1). For example, if the Si content of a glass is held constant at 50 atoms per cent, an increase in the ratio Na^+/Al^{+++} from 1 to 5 progressively shifts selectivity from sequence X to sequence II. Glasses in which the alkali oxide is Li_2O or K_2O rather than Na_2O show qualitatively the same dependence of selectivity on the Li^+/Al^{+++} or K^+/Al^{+++} ratio. In summary, the empirical observations concerning the systematic dependence of glass electrode selectivity on pH and glass composition suggest that selectivity is controlled by the strength of the negative sites, weaker (more screened) sites yielding sequences nearer the free-solution mobility sequence.

Similar observations suggesting the control of selectivity by negative charge strength have been reported for a biological membrane by Wright & Diamond (16, 44). They estimated relative ionic permeability coefficients in rabbit gallbladder epithelium from measurements of the transepithelial diffusion potentials resulting from ion concentration gradients. At pH 7 the epithelium was more permeable to cations than to anions (e.g., a dilute solution of KCl went electrically positive to a concentrated solution), which suggests that the epithelial cell membranes bore a net negative charge (possibly carboxyl or phosphate groups). At pH 2.4, which the epithelium withstood well providing the exposure was brief, the dilute solution of KCl went electrically negative rather than positive, which indicates that permeability to anions was now higher than to cations and suggests that the membrane bore a net positive charge (possibly amino groups). Variation of pH in the range 2.4 to 10 yielded a graph of KCl diffusion potentials against pH [see Figures 1 and 3 (16)] similar to a pH titration curve for an amphoteric substance with an isoelectric point around pH 3. Low pH both reduced cation conductance and increased anion conductance, as one would expect for a membrane with ionizable negative as well as positive groups.

This picture of the gall bladder as an amphoteric membrane was reinforced by two other kinds of observations: calcium reduced cation conductance and increased anion conductance, presumably by binding membrane negative charges and by acting as a positive site for anion exchange; and

exposure to 1,5-difluoro-2,4-dinitrobenzene, which removes positive charge by reacting with amino and other groups, decreased the ratio P_{Cl^-}/P_{Na^+} at low pH. Thus, the strength of the membrane charges responsible for ion selectivity could be monitored by measurements of KCl diffusion potentials and manipulated by changes in pH. Measurement of alkali-cation permeability ratios as a function of pH, based on bi-ionic potentials, yielded two conclusions: 1. The permeability sequence for alkali cations was $K^+ > Na^+ > Cs^+$ (sequence V or VI) at pH 7 but was $K^+ > Cs^+ > Na^+$ (sequence III or IV) at pH 2.4. Thus, a Na^+–Cs^+ inversion occurs between pH 2.4 and 7. 2. The ratio P_{K^+}/P_{Na^+}, while it did not invert, was considerably greater than the free-solution mobility ratio at pH 7 and decreased towards the free-solution value with decreasing pH. This shift of alkali-cation selectivity in a simple biological membrane towards free-solution sequences and values when membrane negative charges are screened by protons is analogous to the behavior of the glass electrodes. It happens that the inversions observed in the gallbladder are duplicated in detail by a glass electrode with the composition 28.3 per cent Na_2O–9.7 per cent Al_2O_3–62.0 per cent SiO_2. Undoubtedly the same phenomenon underlies the observation (45) that the relative potencies of Li^+, Na^+, and K^+, measured electrophoretically, in blocking the negative charges of colloidal trioxystearate and hexaoxystearate shift from sequence X or XI to sequence VI or lower as pH is decreased from 10 to 6.

Thus, these observations on the glass electrodes, on a biological membrane, and on colloids suggest that variation in negative charge strength is what primarily controls alkali-cation selectivity. How does this control operate? Eisenman's reconstruction (1, 2) is based on three facts: 1. Equilibrium cation specificity depends, by definition, upon the free energy difference between ion:membrane and ion:water interactions. 2. Free energies of interactions involving the alkali cations depend largely upon electrostatic forces. 3. The observed selectivity patterns imply that the principal electrostatic forces involved in most systems studied are Coulomb forces (i.e., the forces between two nonpolarizable point charges, varying as the inverse square of the distance). The first two of these statements are self-evident truisms, while the third is an empirical observation which need not apply to all systems.

Consider a material with negative charges,[3] in contact with an aqueous solution containing different alkali cations. The cation preferred by the

[3] The material need not have *net* negative charge: for energetic reasons the nearest neighbor of an alkali cation in biological and many nonbiological systems is at most times certain to be some negatively charged oxygen atom, either in a water molecule, or else in a carboxyl, phosphate, aluminosilicate, or other group. The principles of equilibrium selectivity are the same whether the negative charge is on a biological membrane, an enzyme, an active transport "carrier", a glass electrode or other ion exchange membrane, or a clay or mineral. Relations between nonequilibrium selectivity (e.g., mobility differences) and equilibrium selectivity are discussed on p. 610.

negative site as its nearest neighbor will be that cation which experiences the greatest decrease in free energy when its nearest neighbor becomes the site rather than water. In general, the relative affinities of the site for two different cations a and b will be governed by the free energy difference

$$\Delta F_{a,\,\text{site}} - \Delta F_{b,\,\text{site}} - \Delta F_{a,\,\text{water}} + \Delta F_{b,\,\text{water}} \qquad 1.$$

where $\Delta F_{a,\text{water}}$ and $\Delta F_{b,\text{water}}$ are the free energies of hydration and $\Delta F_{a,\text{site}}$ and $\Delta F_{b,\text{site}}$ are free energies of interaction between the cation and the negative site. Consider now two extreme cases. Suppose that the site has a very high electric field strength, so that cation:site attractive forces and ΔF's, and their differences, are much higher than the hydration energies and their differences. Then affinities will be controlled by $\Delta F_{a,\text{site}} - \Delta F_{b,\text{site}}$. The smallest cation will have its center of charge nearest the site and will experience the largest attractive force, which for a strong site outweighs its also having the highest free energy of hydration, so that affinity will decrease with increasing ionic radius and sequence XI ($Li^+ > Na^+ > K^+ > Rb^+ > Cs^+$) is obtained. Suppose on the other hand that the site has a very low electric field strength, so that ion:site attractions are much weaker than hydration energies. Then expression 1 is dominated by $\Delta F_{a,\text{water}} - \Delta F_{b,\text{water}}$, the difference in free energies of hydration. In this case the smallest cation, which has the highest free energy of hydration, will have the most unfavorable value of $\Delta F_{\text{ion, site}} - \Delta F_{\text{ion, water}}$ so that affinity will decrease with decreasing ionic radius (increasing apparent hydrated size) and sequence I ($Cs^+ > Rb^+ > K^+ > Na^+ > Li^+$), the lyotropic series, is obtained. These two extreme cases would correspond to glasses with low or high alkali oxide content, or to glasses or membranes at high or low pH.

As site strength is varied continuously from a very low to a very high value, one expects selectivity to proceed through transition sequences which must be calculated from the ΔF's of expression 1. Differences between ΔF's of hydration are accurately known experimentally (46, 47). Eisenman (1, 2) employed two methods of obtaining $\Delta F_{\text{ion, site}}$ for sites of different strengths. Both methods used the alkali halides as examples of anionic sites with different field strengths: the four halide anions (F^-, Cl^-, Br^-, I^-) differ from each other to a first approximation only in size, so that the strongest electrostatic attractive forces for a cation would be exerted by the small F^-, which consequently behaves as a site with high effective field strength; while the weakest attraction would be exerted by the large I^-, whose effective field strength is consequently low. The first method of estimating $\Delta F_{\text{ion,site}}$ for halide-type sites of different field strengths was therefore to equate these ΔF's with the experimentally determined free energies of formation of the alkali halides (NaF, RbCl, KBr, etc.), either as the diatomic gases, or as the crystals, or in aqueous solution (from activity coefficients and osmotic coefficients). This thermochemical method thus used empirical quantities without making assumptions about the forces responsible for these ΔF's. The second method was to apply Coulomb's law to a system consisting of a

negatively charged sphere of variable radius and a positively charged sphere of radius equal to the ionic radius of one of the alkali cations. This method assumes that non-Coulombic forces make only a minor contribution to the free energy, an approximation that is valid for alkali cations and halide sites. The Coulomb calculation was carried out both for a system with widely separated sites (such as a diatomic gas) and for a system with sites at the minimum possible distance (such as an alkali halide crystal), in the latter case taking account of the Madelung constant derived from crystal geometry (see p. 609 for the effect of site spacing). Both the thermochemical and the Coulomb methods yield curves of $(\Delta F_{\text{ion, site}} - \Delta F_{\text{ion, water}})$, as a function of the site field strength or the radius of the halide ion, for each of the five alkali cations. These curves repeatedly intersect each other, the intersections determining transitions from one selectivity sequence to another. Both the thermodynamic method and the Coulomb approximation yield essentially the same nine transition sequences (see 1, Figures 16, 17, 18, 20), which are found to be the same as those consistently observed in biological and nonliving systems and listed on p. 585. The intuitive explanation why these particular transition sequences are obtained is discussed on p. 606.

While these model calculations varied the radius of a halide-type site to produce different field strengths and hence different selectivity sequences, the sites in most biological systems will be either carboxyl or phosphoric acid groups, so that only two different values of actual site radius should occur biologically despite the wide range of biological selectivity sequences. However, the field strength (hence the selectivity pattern) of carboxyl and phosphate groups will vary greatly, depending upon whether inductive effects exerted by the site's immediate molecular environment increase or decrease electron density on the site. This influence of the environment upon the field strength of a given chemical grouping is reflected not only in counterion selectivity patterns but also in the much more familiar variation in the acid dissociation constant or pK_a of the site. The pK_a depends upon field strength because an anionic site with high field strength binds protons more firmly than one with low field strength, hence the protons dissociate less readily and the stronger site has a lower dissociation constant and higher pK_a (is a "weaker" acid). As is well known, the pK_a of a given grouping is intimately dependent upon the chemical environment: for instance, the pK_a of the carboxyl group in acetic acid is 4.75 but is 0.70 in trichloroacetic acid because of the electron-withdrawing effect of the chlorines on the carboxyl oxygens. Further examples are provided by the frequently large differences between the pK_a's of free amino acids and their values in proteins.

This relation between pK_a and field strength is important in that it offers the possibility of predicting the pK_a of membrane sites controlling ion selectivity from the observed selectivity pattern, and vice versa. Eisenman set out from the known pK_a's of HCl and HF, the known crystal radii of Cl^- and F^-, and the known alkali-cation selectivity patterns of Cl^- and F^-

(from ΔF's of formation of alkali chlorides and fluorides, combined with hydration free energies of the alkali cations). If one assumes a linear relation between pK_a and equivalent site radius, then the two points for Cl^- and F^- determine a straight line from which pK_a's corresponding to other values of equivalent site radius (hence other selectivity patterns) can be read off [cf. Figure 7, ref. (2)]. Tests of these predictions can be made from experiments on the gallbladder and on glass electrodes. The graph of KCl diffusion potentials against pH in the gallbladder [Figure 3, ref. (16)] implies that the sites for cation exchange in gallbladder cell membranes have a pK_a near 3. From the relation determined by Cl^- and F^-, a pK_a of 3 for widely spaced sites implies cation selectivity sequence VII approaching sequence VI. The actual sequence obtained from bi-ionic potentials in the gallbladder (16) is $K^+ > Na^+ > Cs^+$, which implies either selectivity sequence VI or else V, in satisfactory agreement with the prediction. The observed selectivity patterns of glass electrodes also agree well with predictions based on pK_a's of their ion exchange sites and on the Cl^--F^- relation (1). Correlations between ion selectivity patterns and pK_a's had already been noticed empirically, though not understood theoretically, by Jenny (9) in 1932 when he studied different soil minerals and by Bregman (48) in 1953 when he investigated different organic ion exchange resins. If one applies the same considerations to the selectivity change underlying action potentials in nerve, this change can be interpreted in two ways: cations may cross nerve membranes via the same channels in the active as in the resting state, but a change in the molecular environment during the rising phase of the action potential inductively modifies the charges in the channels so that they acquire a higher field strength and higher pK_a; or else (perhaps more likely), during the rising phase of the action potential a new set of channels is opened, whose charges have a higher pK_a than those controlling ion permeation in the resting state.

Anion Selectivity

Considerations identical to those outlined above for discrimination among the five alkali cations can be extended to the four halide anions (F^-, Br^-, Cl^-, I^-), except that one must consider interactions of negative mobile ions with positive sites instead of positive mobile ions with negative sites. From experimental ΔF's of formation of alkali halides as crystals and in aqueous solution, using the different alkali cations as models of positive sites with different field strengths, Eisenman (3) predicted seven selectivity sequences out of the 24 possible permutations of the four halide anions. We find that application of Coulomb's law to infinitely separated positive sites, or of Coulomb's law times the Madelung constant to closely spaced positive sites, yields the same seven sequences as Eisenman's thermochemical predictions:

I $I^- > Br^- > Cl^- > F^-$

II $Br^- > I^- > Cl^- > F^-$

III $Br^- > Cl^- > I^- > F^-$

IV $Cl^- > Br^- > I^- > F^-$

V $Cl^- > Br^- > F^- > I^-$

VI $Cl^- > F^- > Br^- > I^-$

VII $F^- > Cl^- > Br^- > I^-$

Sequence I, the order of the free-solution mobilities, is associated with weak sites, while sequence VII, in which the ion with the smallest nonhydrated radius is preferred, arises at strong sites. Five transition sequences link I to VII. As one proceeds from I to VII, the first inversion involves the weakly hydrated I^- and Br^-, which have the largest ionic size; the next inversions (II→III, III→IV) involve the more strongly hydrated Cl^-; and the remaining inversions involve F^-, the smallest and most strongly hydrated anion.

For comparison with these predictions, 17 instances have come to our attention in which halide selectivity patterns were recently determined in biological systems. The positive sites in biological systems are most likely amino groups, though there are other possibilities. Wherever quantitative information was provided in these publications, we have extracted estimates of relative potencies (taking Cl^- as 1.00) and list these estimated potencies in parentheses next to each ion in the following survey. In all 17 cases the observed pattern is one of the predicted seven sequences:

From effects on the membrane potential of *Ascaris* muscle (49) the order of permeability was deduced to be $I^- > Br^- > Cl^-$ (sequence I).

The anion potency sequence for stimulation of the olfactory receptor in frogs, as judged by surface electrode recording, was determined (50) as $Cl^- > Br^-$, $F^- > I^-$ (sequence V or VI).

Alkali salts of different halides (18) stimulated the salt receptor of the blowfly with the relative potency I^- (1.5) > Br^- (1.2) > Cl^- (1.0) > F^- (0.4) (sequence I).

The conductances induced by γ-aminobutyric acid in the inhibitory postsynaptic membrane of the crayfish neuromuscular junction (51) were reported as Br^- (1.28) > Cl^- (1.00) > I^- (0.87) (sequence III).

The permeability order of the outer surface of bullfrog skin (35) is Br^- (1.06) > Cl^- (1.00) > I^- (0.25) (sequence III).

Efflux rate constants from red blood cells were observed (52) to be in the order Cl^- (1.0) > Br^- (0.2) > F^- (0.1) > I^- (0.02) (sequence V), and equilibrium concentration ratios in the order I^- (1.82) > Br^- (1.09) > Cl^- (1.00) > F^- (0.86) (sequence I).

From permeabilities determined for the nonsynaptic membrane of cat motoneurons from recovery of the inhibitory postsynaptic potentials after intracellular injection of various salts (53), one obtains the permeability order Br^- (1.26) > Cl^- (1.00) > I^- (0.67) (sequence III).

The order $I^- > Br^- > Cl^-$ (sequence I) is obtained for abilites to diminish the electrophoretic velocity of three positively charged proteins discussed by Bungenberg de Jong (28): casein (2.96, 1.7, 1.0), gelatin (2.24, 1.59, 1.0), and clupein.

The order of anion conductances in cardiac muscle is $I^- > Br^- > Cl^-$ (sequence I) (54). The reverse order, Cl^- (1.00) > Br^- (0.67) > I^- (0.44) (sequence IV or higher), holds for the anion conductances of frog skeletal muscle (55).

The bi-ionic potentials reported (56) for thin lipid membranes treated with the polyene antibiotic nystatin imply the permeability order Cl^- (1.00) > I^- (0.80) > F^- (0.38) (sequence III or IV).

Observations (57) on the abilities of internally perfused halide ions to block conduction in squid axons lead to the permeability order I^- (5.55) > Br^- (1.61) > Cl^- (1.00) > F^- (0.23) (sequence I).

Anions potentiate the contracture of vascular smooth muscle (58) in the order I^- (1.75) > Br^- (1.25) > Cl^- (1.00) (sequence I).

The enzyme carbonic anhydrase is inhibited by halides (59) in the order of decreasing inhibition I^- (22.2) > Br^- (2.5) > Cl^- (1.0) > F^- (0.8) (sequence I).

From these experimental values for relative potencies, the halide selectivity isotherms of Figure 1 have been constructed by plotting the relative potency of each halide ion on the ordinate scaled according to the I^-/Cl^- potency ratio on the abscissa. It is apparent that the experimental numbers determine four curves, intersections between which correspond to transitions from one sequence to another. The fact that a regular pattern is observed means simply that once one knows the I^-/Cl^- selectivity ratio, one not only can predict qualitatively the whole halide sequence but also quantitatively the approximate relative potencies for F^- and for Br^-. For instance, in the nonsynaptic membrane of cat motoneurons and in the GABA-treated inhibitory postsynaptic membrane of crayfish neuromuscular junction, where the F^- was not tested in the published studies, F^- should prove to be less potent than the other three halogens and roughly 30 per cent as potent as Cl^-.

It will be recalled that the alkali-cation selectivity pattern of an anionic site can be predicted from its acid dissociation constant, since both selectivity pattern and pK_a are related to field strength (p. 594). Similarly, the halide selectivity pattern of a positively charged site should be predictable from its pK_b, a strong site (e.g., halide sequence VII) being associated with a high pK_b. Two kinds of positive sites must be distinguished, which may be written as M^+ and MH^+. In biological systems quaternary ammonium groups provide examples of M^+ sites, and the alkali cations serve as inorganic models. For the MH^+ site the biological representatives would be primary, secondary, and tertiary amino groups, and NH_4^+ ($pK_b = 4.75$) serves as an inorganic model. Calculations similar to those published by Eisenman (2) for anionic sites lead us to the conclusion that an M^+ site exhibits a much higher halide selectivity sequence than an MH^+ site with the same pK_b and site spacing; and that only sequence VII should result from any M^+ site with $pK_b > 0.7$ ($pK_a < 13.3$), even at infinite spacing. Thus, the fact that erythrocyte anion permeability is sequence V (52) and that the positive charges controlling the permselectivity of erythrocytes appear to

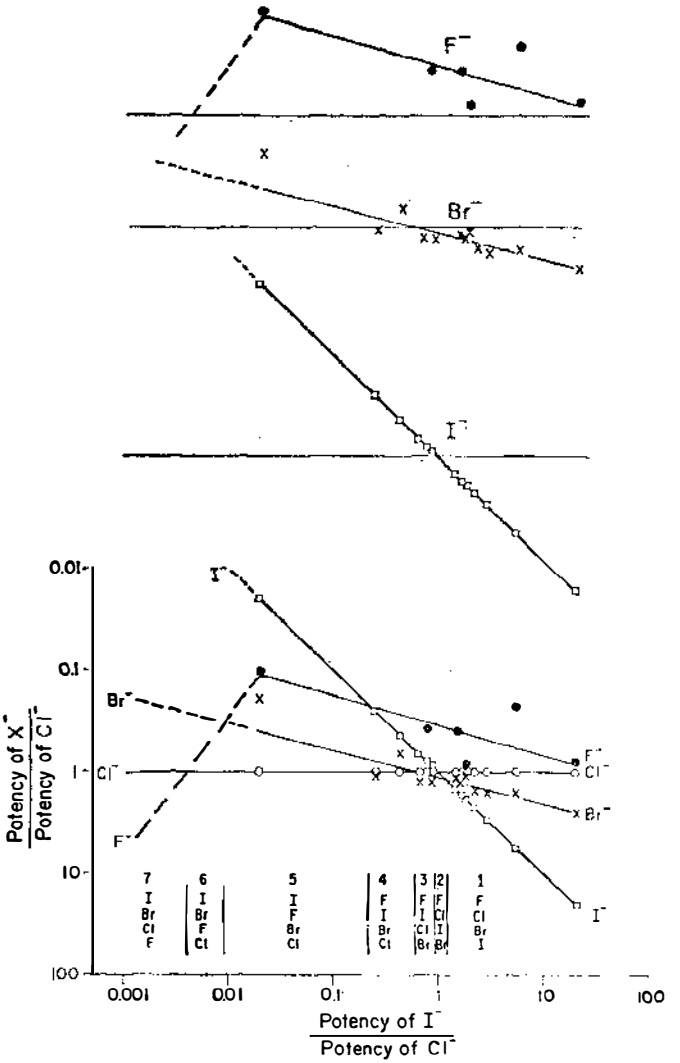

FIG. 1. Below, selectivity isotherms for the halide anions in biological systems. Each set of four points arranged vertically above each other is one of the relative potency sequences experimentally measured in a biological system and listed on pp. 595–96 (●F^-, ○Cl, XBr^-, □I^-). The potencies relative to $Cl^-=1$ are plotted logarithmically on the ordinate. They are arranged according to the relative I^- potency, plotted logarithmically on the abscissa. [For instance, halides inhibit the enzyme carbonic anhydrase (59) with the relative potencies $I^-=22.2$, $Br^-=2.5$, $Cl^-=1.0$, $F^-=0.8$. These points have therefore been arranged on an imaginary vertical line intersect-

have $pK_b = 5$ means that these charges are not quaternary ammonium groups but belong to the MH^+ type.

Divalent-Cation Selectivity

The divalent cation calcium is important in many biological systems in controlling permeability to monovalent ions, and plays a direct role in generating action potentials in some crustacean nerves and muscles. Of the four alkaline-earth cations (magnesium, calcium, strontium, and barium), all of which are rather similar in their physical and chemical properties, one other, magnesium, occurs naturally in biological systems and is generally found to be very different from calcium in its biological effects. The problem of alkaline-earth selectivity is therefore one whose physical interest and biological importance is second only to that posed by the alkali ions.

A simplified theory of alkaline-earth equilibrium selectivity has been developed independently by Sherry (5), by Truesdell (6, 60), and by Eisenman (3). As in Eisenman's treatment for monovalent cations, specificity in these models is controlled by the field strength of membrane negative charges with which the cations interact. The driving force underlying selectivity is the difference between the free energy of cation:site interaction and the cation's free energy of hydration, and contributions of non-Coulomb forces to cation:site interactions are neglected. Two principal kinds of conclusions emerge from these treatments:

1. The relative affinities of a site for monovalent and for divalent cations depend critically upon intersite spacing: widely spaced sites prefer monovalent to divalent cations, while closely spaced sites prefer divalent cations. Previously, physical chemists had anticipated that the more highly charged

---

ing the horizontal axis at 22.2, and constitute the set of points lying furthest to the right. Since the ordinate gives potency relative to Cl^- as a function of the relative I^- potency on the abscissa, the Cl^- value of 1.0 automatically falls on a horizontal line intersecting the ordinate at 1.0, and the I^- value of 22.2 automatically falls on the line of 45° slope. The Br^- value of 2.5 and the F^- value of 0.8 have been used in constructing the empirical isotherms for these two ions, drawn by eye through all the Br^- or F^- points.] The intersections of these four experimental isotherms represent transitions among seven sequences predicted theoretically by Eisenman and listed below the pattern and numbered 1 through 7 (the most potent ion is written on the bottom in each case). Above, the F^-, Br^-, and I^- isotherms are replotted separately for clarity. In the absence of experimental data for sequences higher than sequence 5, the isotherms have been extrapolated towards the left to show the theoretical predictions that F^- will cross the Br^- and then the Cl^- isotherm. The meaning of the regular pattern is that once the relative potencies of two halides are known, the whole sequence and the approximate potencies of the other two halides can be predicted. For instance, reading vertically upwards from 0.1 on the abscissa, a system in which I^- is one tenth as potent as Cl^- should be in sequence 5 ($Cl^- > Br^- > F^- > I^-$) and should have a F^- potency of about 0.2 and a Br^- potency of about 0.6 relative to Cl^-.

ion should always be preferred and had been surprised to find monovalent ions actually preferred over divalents in some zeolites (61). The zeolites preferring monovalent cations have low site densities (widely spaced sites), while those preferring divalent cations have closely spaced sites, in accord with the theoretical prediction. In principle this fact opens the possibility of estimating site spacings for those biological membranes in which calcium and its analogues are known to displace sodium and potassium.

2. Sherry predicted for closely spaced sites that out of the 24 possible permutations of the four alkaline-earth cations, only seven should be observed as selectivity sequences.[4] These are:

I	$Ba^{++} > Sr^{++} > Ca^{++} > Mg^{++}$
II	$Ba^{++} > Ca^{++} > Sr^{++} > Mg^{++}$
III	$Ca^{++} > Ba^{++} > Sr^{++} > Mg^{++}$
IV	$Ca^{++} > Ba^{++} > Mg^{++} > Sr^{++}$
V	$Ca^{++} > Mg^{++} > Ba^{++} > Sr^{++}$
VI	$Ca^{++} > Mg^{++} > Sr^{++} > Ba^{++}$
VII	$Mg^{++} > Ca^{++} > Sr^{++} > Ba^{++}$

Sequence I, the order of the free-solution mobilities, arises at weak sites, where the free energy of hydration dominates exchange; but sequence VIII, in which the ion with the smallest ionic radius is preferred, arises at strong

[4] The sequences predicted by Truesdell and by Eisenman differ from those of Sherry and disagree with those observed experimentally in biological systems. We have repeated the calculations, and find that the predictions differ because Truesdell neglected entropy changes, equating free energy with enthalpy, while Sherry took estimated entropies of hydration into account; and that Sherry used the Goldschmidt radii for the alkaline-earth ions, while Truesdell used Green-Evans radii and Eisenman used Pauling radii. The Goldschmidt radii are the more appropriate ones, since they were derived from oxide crystals and the biological sites are oxygen sites. Sequences obtained from a number of minerals, resins, and glasses [summarized in Table 11–3, (6)] do conform to Truesdell's predictions and differ from the experimental biological sequences. However, almost all of the biological studies cited on pp. 601–2 involve measurements of equilbrium selectivity without a mobility component (cf. p. 610), whereas the mineral and glass patterns for divalent cations may be controlled by mobility differences rather than reflecting equilibrium selectivity, since mobilities of divalent cations in glasses and minerals are far below those of monovalent cations (6). For his calculations Sherry extracted free energies of hydration of the four alkaline-earth ions from the thermal data of Rossini et al. (46) by assuming that the entropy of ionization in the gas phase is the same for all four ions. The resulting free energies of hydration are very close to those estimated recently by Rosseinsky (47); Rosseinsky's values lead to prediction of the same specificity patterns. Sherry suggested that infinitely spaced anionic sites yielded only the lyotropic series, but he did not carry his calculation below an equivalent site radius of 0.8 Å. For infinitely spaced sites with smaller radii (higher field strengths) we find that the predicted selectivity pattern is virtually the same as for closely spaced sites, except that sequence III becomes $Ba^{++} > Ca^{++} > Mg^{++} > Sr^{++}$.

sites, where ion: site interactions are stronger than free energies of hydration. In addition, a selectivity shift in the direction VII to I occurs with increasing site spacing at constant field strength, as also found for alkali-cation selectivity (see p. 609).

The agreement between Sherry's predicted sequences and those recently observed experimentally in biological systems is substantial. Wherever quantitative information was available, the potencies relative to $Ca^{++}=1.0$ which we extracted are given in parentheses:

Bungenberg de Jong (28) summarized the results obtained by himself and by several other authors in so-called reversal-of-charge experiments on the electrophoretic mobility of proteins and of phosphate, carboxyl, and sulfate colloids of biological origin. The underlying principle is that the relative potencies of different cations in blocking negative charges on amphoteric colloids are determined by finding the concentration of cation necessary to reverse the charge of the colloid (the more potent the cation, the lower this concentration). Of the 19 systems discussed by Bungenberg de Jong, 18 yielded sequences predicted by Sherry, and five of the seven Sherry sequences are represented. The details are: $Ba^{++}>Sr^{++}>Ca^{++}>Mg^{++}$ (sequence I), the carboxyl colloids arabinate (1.64, 1.38, 1.00, 0.85), pectinate (2.90, 1.25, 1.00, 0.79), and pectate (2.08, 1.18, 1.00, 0.80), the sulfate colloids chondroitin sulfate (1.37, 1.16, 1.00, 0.85), agar (6.67, 2.17, 1.00, 0.74), and carrageen (1.59, 1.35, 1.00, 0.93), the colloids SiO_2 (1.56, 1.06, 1.00, 0.93) and TiO_2 (4.0, 1.2, 1.0, 0.7); $Ba^{++}>Ca^{++}>Sr^{++}>Mg^{++}$ (sequence II), the carboxyl colloid hexaoxystearate at pH 6 and the phosphate colloid nucleate (1.23, 1.00, 0.91, 0.81); $Ca^{++}>Ba^{++}>Sr^{++}>Mg^{++}$ (sequence III), the phosphate colloid soya bean phosphatide II (1.00, 0.90, 0.74, 0.59); $Ca^{++}>Mg^{++}>Ba^{++}>Sr^{++}$ (sequence V), the protein gelatin and the phosphate colloid egg lecithin+50 per cent cholesterol (1.00, 0.66, 0.30, 0.26); $Ca^{++}>Mg^{++}>Sr^{++}>Ba^{++}$ (sequence VI), the protein casein, the carboxyl colloid trioxystearate at pH6, and the phosphate colloids egg lecithin (three different preparations: 1.00, 0.52, 0.14, 0.12; 1.00, 0.49, 0.13, 0.11; 1.00, 0.70, 0.29, 0.22), sphingomyelin (1.00, 0.27, 0.08, 0.055), and soya bean phosphatide I (1.00, 0.73, 0.35, 0.26); and $Mg^{++}>Ca^{++}>Sr^{++}>Ba^{++}$ (sequence VII), the carboxyl colloids oleate (1.85, 1.00, 0.93, 0.81) and trioxystearate at pH10. Hexaoxystearate at high pH yielded $Mg^{++}>Ca^{++}>Ba^{++}>Sr^{++}$, which differs from sequence VII in that Ba^{++} has recrossed Sr^{++} (see discussion of "post-Coulomb sequences", pp. 603 and 607). More recently, Bangham, Pethica & Seaman (62) have confirmed Ca^{++} (1.00) $>Sr^{++}$ (0.36) $>Ba^{++}$ (0.14) (VI or VII; Mg^{++} not tested) for egg lecithin.

Bungenberg de Jong's results are also important in showing that the selectivity pattern for divalent cations shifts with decreasing pH (decreasing field strength) in the direction from the strong-field sequence VII to the weak-field sequence I, as discussed for the effects of pH on monovalent-cation selectivity (pp. 591–92). This is seen in the effect of pH on the charge reversal patterns of oleate and trioxystearate.

Wright & Diamond (16) compared the potencies of the alkaline earths in blocking membrane negative charges in the gallbladder, as measured by the decrease in NaCl diffusion potentials and hence in P_{Na}/P_{Cl} caused by the addition of a divalent cation at 5mM. The potency order was Ba^{++} (1.13) > Ca^{++} (1.00) > Sr^{++} (0.61) > Mg^{++} (~0) (sequence II) in three gallbladders, Ca^{++} (1.00) > Ba^{++} (0.84) > Sr^{++} (0.57) > Mg^{++} (~0) (sequence III) in nine other gallbladders. Presumably the sites were stronger or more closely spaced in the latter preparations.

Goldner, Cassidy & Tidball (63) compared the alkaline earths in their ability to restore the normal permeability properties of the intestine after treatment with EDTA and obtained Mg^{++} (1.25) > Ca^{++} (1.00) > Sr^{++} (0.50) > Ba^{++} (0.29) (sequence VII).

Effects on the rate of rise of the spike in barnacle muscle were shown by Hagiwara & Takahashi (64) to be in the order $Ca^{++} > Mg^{++} > Sr^{++}$ (Ba^{++} not tested; sequence IV, V, or VI).

Peak transient membrane currents in the alga *Chara australis* (65) are stimulated in the sequence Ca^{++} (1.00) > Sr^{++} (0.8) > Mg^{++} (~0), Ba^{++} (~0). This is not a Sherry sequence but is nearest VI, differing in the low potency of Mg^{++}.

Ability to replace calcium in reactivating the enzyme Taka amylase A (66) is in the order Mg^{++} (1.17) > Sr^{++} (1.04) > Ca^{++} (1.00) > Ba^{++} (0.95). This order is also not a Sherry sequence but is nearest VII, differing in the reversed positions of Sr^{++} and Ca^{++} (see discussion of post-Coulomb sequences, pp. 603 and 607).

Ponder (67) noted that red cells incubated in solutions of the alkaline-earth chlorides at 4° C lost K^+ in exchange for divalent cations. The extent of K^+ loss is a measure of the divalent-cation permeability and yields the sequence $Ca^{++} > Ba^{++} > Mg^{++} > Sr^{++}$ (sequence IV).

The order of the apparent binding constants of the alkaline earths with the protein G-actin (68) is Ca^{++} (1.00) > Mg^{++} (0.25) > Sr^{++} (0.03), Ba^{++} (0.01) (sequence V or VI).

The amounts of divalent cations bound to reconstituted collagen (69) are in the order Mg^{++} (1.68) > Ca^{++} (1.00) > Sr^{++} (0.79) (sequence VII).

Stimulating effects of alkaline earths on peak sodium and potassium conductance of squid axon (70) follow the sequence $Ba^{++} > Ca^{++} > Mg^{++}$ (sequence I or II).

Thus, all of the Sherry sequences have been observed in biological systems, and 27 of the 30 reported experimental sequences fit the Sherry patterns.

From these experimental values for relative potencies, the alkaline-earth selectivity isotherms of Figure 2 have been constructed by plotting the relative potency of each ion on the ordinate scaled according to the Ba^{++}/Ca^{++} potency ratio on the abscissa. The experimental potencies cluster closely about four curves, intersections between which correspond to transitions from one sequence to another. The fact that a regular pattern is observed

means simply that once one knows the relative potencies for two ions, one not only can predict qualitatively the whole alkaline-earth sequence but also quantitatively the approximate relative potencies of the other two ions. For example, as regards binding to reconstituted collagen, where the published study did not test Ba^{++}, Ba^{++} should prove to be bound less strongly than the other three alkaline-earth ions and roughly 60 per cent as strongly as Ca^{++}.

The experimental isotherms of Figure 2 have maxima, so that a given value of Ba^{++}/Ca^{++} may correspond to either of two sequences and sets of selectivity ratios. It is obvious that if the isotherms are extrapolated in the high-field-strength direction (towards the left) beyond sequence VII, the isotherms for the two largest ions Ba^{++} and Sr^{++} will recross the Ca^{++} isotherm, giving rise to a new set of sequences not predicted by the Coulomb model. Two out of the three non-Sherry sequences from the recent experimental literature (hexaoxystearate at high pH, and Taka amylase A) in fact belong to this new series. An analogy is encountered in alkali-cation selectivity, where the isotherms also have maxima (3, Figure 7) and a new set of sequences not predicted by the Coulomb model appears at very high field strengths, beginning with recrossings by Rb^{+} and Cs^{+}, the two largest ions. The same may prove true of the halide isotherms, but the available experimental data have not yet included high-field-strength sequences (halide sequences VI and VII) where the maxima would become apparent. This appearance of post-Coulomb sequences at high field strengths is to be expected from simple electrostatic considerations involving non-Coulomb forces, as will be discussed on pp. 606–7.

Other Ions

Polyvalent cations other than the alkaline earths, such as La^{+++}, the transition-metal ions (Mn^{++}, Fe^{++}, Co^{++}, Ni^{++}, Cu^{++}, etc.), Al^{+++}, and the actinides $(UO_2)^{++}$ and Th^{++++}, mimic the effects of calcium to varying extents in several biological systems. Apparent potency sequences have been determined for polyvalent cation effects on the calcium spike of barnacle muscle (64), on reducing sodium conductance and increasing chloride conductance in gallbladder (16), on the electrophoretic mobility of colloids (28), and on Na^{+} and K^{+} conductances in squid axon (70). Some biological potency sequences for monovalent inorganic ions other than the alkali metals and halogens (e.g., Ag^{+}, Tl^{+}, NH_4^{+}, NO_3^{-}) and for monovalent organic ions have also been obtained.

Whereas analyses based solely on Coulomb forces usually predict successfully the behavior of the alkali cations, the halides, and the alkaline earths, non-Coulomb forces cannot be disregarded for other ions, which have received little theoretical attention because of the resulting complexities [see (13), Figures 51 and 52 for theoretical Ag^{+}, Tl^{+}, and NH_4^{+} isotherms]. In addition, it is frequently not appreciated that many polyvalent cations undergo transformation reactions (hydrolysis, oxidation, and complex

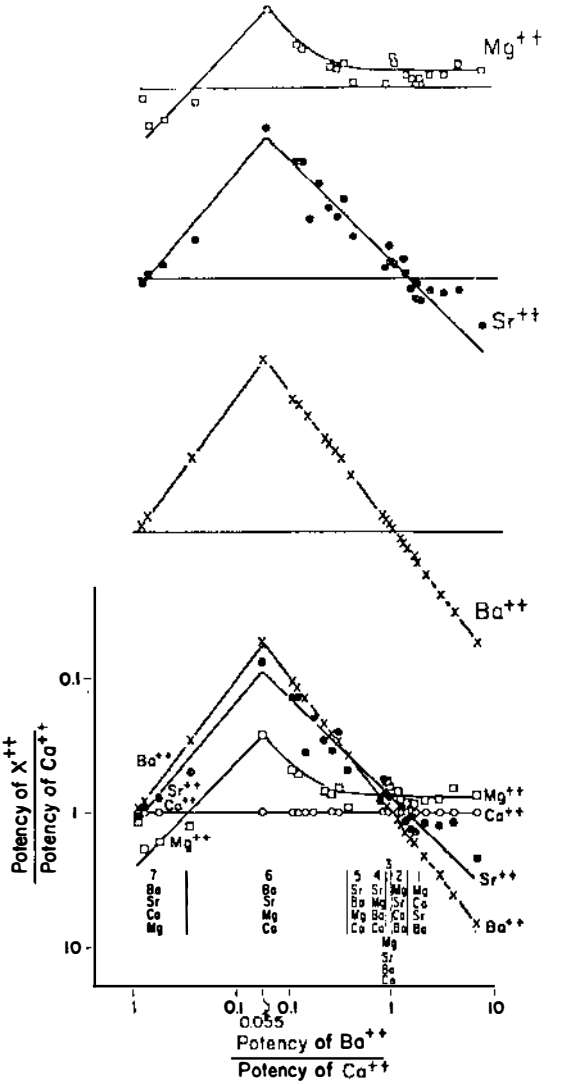

FIG. 2. Below selectivity isotherms for the alkaline-earth cations in biological systems. Each set of four points arranged vertically above each other is one of the relative potency sequences experimentally measured in a biological system and listed on p. 600 (□Mg^{++}, ○Ca^{++}, ●Sr^{++}, ×Ba^{++}). The potencies relative to $Ca^{++}=1$ are plotted logarithmically on the ordinate. They are arranged according to the relative Ba^{++} potency, plotted logarithmically on the abscissa. [For instance, alkaline-earth cations reverse the charge of colloidal agar (28) with the relative potencies $Ba^{++}=6.67$, $Sr^{++}=2.17$, $Ca^{++}=1.00$, $Mg^{++}=0.74$. These points have therefore been arranged on an imaginary vertical line intersecting the horizontal axis at 6.67, and con-

formation) in aqueous solution, some of which cause large shifts in pH (cf. 16). Thus, biological effects reported for such ions as Cu^{++} and Al^{+++} are not due to these ions themselves but to their transformation products, and must even be suspected of resulting from pH changes in cases where these were not specifically ruled out. For instance, the apparent effect of Cu^{++} on anion permeability in frog skin (71) and other epithelia is probably actually due to interaction of the anion $(CuCl_4)^{--}$, the most stable form of copper in $CuCl_2$ solutions (72), with membrane positive charges.

Non-Coulomb Forces, and the Meaning of the Transition Sequences

Having considered in broad outline the basis of equilibrium ion selectivity, we now examine in more detail the effects of some variables related to selectivity, beginning with non-Coulomb forces (forces other than those between two point charges or monopoles).

The thermochemical method of calculating ion selectivity sequences makes no assumptions about the relative contributions of enthalpy and entropy terms, nor about the relative contributions of Coulomb and non-Coulomb forces, to the free energy of ion-site interaction. Alkali cations and halide anions interacting with each other can in fact be well approximated as monopolar charges on spherical, nonpolarizable particles, and it is therefore not surprising that the thermochemical method and the calculations based solely on Coulomb forces have yielded the same alkali-cation selectivity sequences when applied to halide-type sites.

What is the reason for the particular pattern of transition sequences predicted by the Coulomb model? As discussed on p. 586, the pattern was that inversions involving the large Cs^+, Rb^+, and K^+ occurred first, those involv-

---

stitute the set of points lying furthest to the right. Since the ordinate gives potency relative to Ca^{++} as a function of the relative Ba^{++} potency on the abscissa, the Ca^{++} potency of 1.00 automatically falls on a horizontal line intersecting the ordinate at 1.00, and the Ba^{++} value of 6.67 automatically falls on the line of 45° slope. The Sr^{++} value of 2.17 and the Mg^{++} value of 0.74 have been used in constructing the empirical isotherms for these two ions, drawn by eye through all the Sr^{++} or Mg^{++} points.] The significance of the observed regularity is that once one knows the relative Ba^{++} potency, one not only can predict qualitatively the whole alkaline-earth sequence but also quantitatively the approximate relative potencies. For instance, reading vertically upwards from 2 on the abscissa, a system in which Ba^{++} is twice as potent as Ca^{++} should be in sequence 1 ($Ba^{++} > Sr^{++} > Ca^{++} > Mg^{++}$) and should have a Sr^{++} potency of about 1.3 and a Mg^{++} potency of about 0.7 relative to Ca^{++}. The degeneracy of the abscissa and the maxima in the isotherms mean that a given Ba^{++} potency may correspond to either of two sequences and relative potencies. The intersections of these four experimental isotherms determine seven sequences predicted theoretically by Sherry and listed below the pattern (the most potent ion is written on the bottom in each case). Above, the Mg^{++}, Sr^{++}, and Ba^{++} isotherms are replotted separately for clarity.

ing the smaller Na^+ next, and those involving the smallest ion Li^+ last, as one proceeded from the case (sequence I) where ion-site attractions were much weaker than hydration energies to the case (sequence XI) where they were much stronger. The same pattern is observed in the seven selectivity sequences for halide anions (pp. 595–96).

The underlying reason for these patterns is that cation: halide-site forces decrease more slowly with increasing distance than do cation: water forces. The forces between an alkali cation and a halide anion are largely Coulomb or monopole-monopole forces, which decrease as the inverse square of the distance. The forces between an alkali cation and a multipolar water molecule are largely dipolar and quadrupolar forces, which vary as r^{-3} and r^{-4}, respectively. The difference between the attraction for a small ion (e.g., Li^+) minus the attraction for a large ion (e.g., Cs^+) is therefore less marked for a monopolar site than for a water molecule. As site strength is increased so that ion-site attraction gradually begins to increase in strength relative to ion-water attraction, the expression $(\Delta F_{\text{ion,site}} - \Delta F_{\text{ion,water}})$ goes negative most rapidly for Cs^+ and most slowly for Li^+, hence inversions affecting the largest ions occur first.

The opposite extreme is the case in which ion-site forces decrease more rapidly with increasing distance than do ion-water forces. This would be true, for instance, in the case of a highly polarizable site for which ion: induced-dipole forces (varying as r^{-5}) were more important than for the ion-water case. This greater contribution of polarization energy to $\Delta F_{\text{ion,site}}$ than to $\Delta F_{\text{ion,water}}$ would be largest for the smallest ion Li^+, whose center of charge would be nearest the site (or water) and which would therefore be the most effective ion at polarizing. Hence inversions affecting Li^+ would occur first as one proceeded from sequence I to XI. This case corresponds to the assumption of Bungenberg de Jong (see p. 590) that the relative polarizabilities of the site and water control cation selectivity.

A more general analysis of alkali-cation selectivity encompassing both these extreme cases was made by Ling (43), who calculated site-cation and water-cation interactions for a linear model, taking into account all non-exchange forces, including such non-Coulomb effects as polarization of the ion by the site, polarization of the site by the ion, and Born repulsion forces. Over a range of values for the site polarizability up to 2 Å these detailed calculations yielded the same alkali-cation sequences as those predicted from Coulomb forces alone, while high polarizabilities yielded different sequences (4, 43).

Whether ion-site interactions will be dominated by Coulomb or non-Coulomb forces, and whether ion-site forces will fall off more rapidly or more slowly with distance than ion-water forces, are questions that can be answered for a membrane only if its structure is known. From the properties of aluminosilicate sites it is physically reasonable that a Coulomb model should successfully predict the selectivity sequences observed in minerals and glass electrodes. Different sequences, in which Li^+ inversions occur first and are followed by Na^+ inversions, have been observed in systems with more polariz-

able sites, such as carboxylate ion exchange resins (4) and two of the phosphate colloids studied by Bungenberg de Jong (28). In biological membranes the identity of the groups controlling ion permeation is unknown. The fact that most biological sequences fit the Coulomb pattern implies that the groups are either ionic (acidic groups) or else relatively nonpolarizable permanent dipoles. However, the shift in the biological Li^+ isotherm, and the sequences in which the position of Li^+ is qualitatively anomalous, discussed on p. 589, suggest that non-Coulomb forces related to site polarization by counterions are more important for the permeability-controlling groups in biological systems than for the aluminosilicate sites of zeolites and glass electrodes. Non-Coulomb forces appear to be responsible for the maxima in the alkaline-earth isotherms (Figure 2) and alkali-cation isotherms and for the resulting post-Coulomb sequences. At very high site field strengths, polarization of the counterion by the site can no longer be considered negligible in comparison with Coulomb forces. The largest ions would be the most polarizable, so that a new set of transitions is expected in which the largest ions (Rb^+ and Cs^+, Ba^{++} and Sr^{++}) again become more potent than the smallest ions. The post-Coulomb sequences appearing at high field strengths and cited earlier (p. 589 and p. 603) are in fact of this expected type. For more polarizable ions such as Ag^+, polarization by the site contributes significantly to the interaction energy even at low field strength and results in glass electrodes being much more permeable to Ag^+ than one would predict from a Coulomb model (13).

In brief, then, most observed sequences are those predicted from consideration of Coulomb forces alone; and the occasional deviations from these patterns are those expected from considering in addition the most important non-Coulomb forces.

"Uncharged" Membranes

Much of the experimental work on ion selectivity has been done on ion exchange membranes, and it has been convenient to develop the theory of ion selectivity using the language of ion exchange. By definition an ion exchange membrane is one containing fixed ionic charges to which mobile, oppositely charged ions from the solution serve as counterions. It would be a serious misunderstanding, however, to assume that there must be some totally different explanation for specificity in systems lacking fixed ionic charges: specificity will still be controlled by electrostatic forces, as generalized in the preceding section (i.e., not necessarily just Coulomb forces), whether the negative charge nearest the cation is ionic, on a permanent dipole (or multipole), or on an induced dipole (or multipole), and whether the site is fixed or located on a mobile carrier. For example, in a molecule with carbonyl groups or ether linkages but no carboxyl groups, the carbon–oxygen bonds will in general have permanent (and induced) dipole moments in which the oxygen is negative. The interactions of a cation with such an oxygen will still depend upon the oxygen's field strength and the distance between the cation's and oxygen's centers of charge, just as if the oxygen had

been in a carboxyl group from which a proton had dissociated. If the electric field of the carbonyl or ether group falls off more slowly with distance than does the field of a water molecule, then the same selectivity sequences as predicted by the Coulomb model may be obtained, for the reasons discussed in the preceding section. Recent calculations by Eisenman (73) on a permanent dipolar model yield Coulomb sequence patterns over a considerable range of charge values and spacings. In general, one expects that the Coulomb model will be most successful for those dipoles with the lowest polarizabilities and the largest separation between the positive and negative ends.

These facts are reflected in the recent experience with the classes of macrocyclic compounds that produce spectacular selective increases in the cation permeability of mitochondrial, erythrocyte, and thin lipid membranes (see p. 587). Incorporation of these compounds into high-resistance membranes may increase alkali-cation permeability by several orders of magnitude, the effect being much more marked for some cations than for others. While the class including nigericin and monensin does contain one carboxyl group (in addition to numerous ether and hydroxyl oxygens), the other classes, such as the cyclic polypeptide antibiotics (e.g., valinomycin and the enniatins), the macrolide actins, and the cyclic "crown" polyethers, lack ionizing groups and contain oxygen only in ether, ester, and hydroxyl groups. Nevertheless, both the selectivity patterns and the magnitudes of selectivity observed with these various classes of macrocyclic compounds agree well with the previously established patterns for nonliving and other biological systems, as discussed on p. 587. Although the *permeation mechanism* induced by these compounds is proving of great interest, the above-mentioned agreement provides no reason to believe, and ample reason not to believe, that their mechanism of *selectivity* involves fundamentally new principles. From this point of view it is misleading to think of these molecules as uncharged or neutral: they lack ionic charges but do have dipoles whose negative oxygen end gives rise to the usual patterns of inter-cation selectivity in the usual way.

The same considerations also mean that discussions of ion selectivity which explicitly or implicitly (e.g., 74, 75) neglect electrostatic forces, for example, because the ion is supposed to cross the membrane via an uncharged pore, are based on a physically impossible fiction. Even if ions crossed biological membranes via pores consisting of pure hydrocarbon with no oxygen groups and with only the small (but not nonexistent) permanent dipoles of carbon–hydrogen bonds—a hypothesis that is highly unlikely but not utterly impossible—the ion:induced-dipole forces between the ion and the surrounding hydrocarbon, together with the free energies of hydration, would still control equilibrium selectivity according to expression 1, p. 593.

Degree of Hydration

An increase in the amount of water in the vicinity of the mobile ion and a site of opposite sign reduces the magnitude of selectivity ratios without altering the selectivity sequence [compare Figures 6A, B, C, and D of (2)].

Only those ions in immediate contact with membrane charges without intervening water molecules contribute significantly to selectivity patterns differing from those of free solution, so that "we may, to a first approximation, regard the effect of additional water as merely to 'dilute' the processes giving rise to selectivity" (4, p. 268). This expectation is in accord with the finding that the magnitudes of selectivity in ion exchangers decrease with increased swelling (hydration) of the exchanger. Since the magnitudes as well as the patterns of alkali-cation selectivity observed in biological membranes are comparable to those observed in zeolites, glasses, and collodion membranes, the implication is that both kinds of systems are in comparable hydration states, i.e., that the association between water and charged groups in biological membranes is comparable to that in a crystalline hydrate.

Effect of Site Spacing or Ion Coordination Number

For ions of the same charge, variation in site spacing or in ion coordination number (the number of sites which the ion nearly touches) does not affect the pattern of transition sequences: closer site spacing or higher coordination number merely yields a sequence corresponding to higher field strength [e.g., compare Figures 3C and 3D of (2)]. The intuitive explanation is that one high-strength site exerts the same force as several low-strength sites.

As discussed previously (pp. 599–600), intersite spacing is critical in governing selectivity between a monovalent and divalent ion.

With nondeformable site-bearing molecules, different ions may have different coordination numbers: for instance, alkali cations of different sizes may be in contact with different numbers of carbonyl or ether oxygens in a macrocyclic polypeptide antibiotic or polyether. In the case of deformable macrocyclic compounds the deformation energy required for a compound to achieve the configuration of minimum energy and maximum coordination number with a given ion may contribute significantly to the free energy balance of expression 1, p. 593.

Entropy Effects

In a membrane in which the replacement of one permeating ion by another leads to no change in the structure or hydration state of the membrane, the entropy change in ion exchange should be given by the difference in entropies of hydration, and $\Delta S_{ion,site}$ should be the same for all ions. Sherry (5) has pointed out that entropy changes in the membrane or exchanger phase are sometimes significant in zeolites with high water content. This is due in part to water transfer in or out of the membrane (hence a change in entropy of the transferred water), associated with the exchange of one ion for another.

Nonequilibrium Selectivity

Up to this point we have discussed the application of physical principles only to the problem of equilibrium selectivity. That is, we have asked the

question: given a material (a membrane, enzyme, mineral, etc.) in contact with an aqueous solution containing several similarly charged ions, in what order will these ions be preferred by the material as its nearest neighbor at equilibrium? Some of the effects whose ionic selectivity we wish to explain involve this kind of purely equilibrium problem: for example, the binding constants of an ion exchanger or of DNA or of proteins, the affinities for active transport mechanisms, the ability to stimulate or inhibit an enzyme, and the reversal-of-charge concentration in electrophoresis of colloids. However, other effects whose specificity has been cited actually contain a nonequilibrium component (as a mobility or an interfacial activation energy) in addition to the equilibrium affinity: for example, the permeability of a glass electrode or of a biological membrane or of a thin lipid membrane, as judged from electrical potential differences under concentration gradients, from electrical conductances, or from tracer fluxes. For an ion exchange membrane, for instance, one may write the permeability ratio P_1/P_2 for two ions as $P_1/P_2 = K(u_1/u_2)$, where K is the ion exchange equilibrium constant for the two ions and u_1/u_2, the mobility ratio, is a nonequilibrium parameter (3). What can be said about selectivity involving nonequilibrium parameters?

The empirical fact is that the selectivity sequences we have cited for effects with nonequilibrium components are essentially the same as the selectivity patterns cited for purely equilibrium effects, and are also the same as those predicted from a theoretical consideration of equilibrium selectivity alone. There are two possible explanations: either the nonequilibrium parameters (e.g., mobilities) in a given system differ much less among the various ions than do the equilibrium parameters; or else the nonequilibrium parameters are dependent functions of the equilibrium parameters. In the glass electrodes it has been shown experimentally that both explanations apply (3): a potassium-selective electrode ($P_{K^+}/P_{Na^+} = 10.3$) was found to have $K = 34$ for K^+-Na^+ exchange (K^+ bound 34 times more strongly than Na^+) but $u_K/u_{Na} = 0.3$. Thus, the mobility ratio is in the opposite direction from the binding-constant ratio (the most strongly bound ion is the least mobile, as one might expect) but is much closer to 1, so that it is the equilibrium sequence which determines the permeability sequence. This quantitative comparison between the binding-constant ratio and the mobility ratio provides the answer to the common misconception, "Shouldn't the most strongly bound ion be the least permeable rather than the most permeable?" In the case of lipid bilayers containing uncharged carriers such as macrocyclic antibiotics it has been suggested (23) that the expression $P_1/P_2 = (u_{1s}K_1)/(u_{2s}K_2) \doteq K_1/K_2$ holds where K is an association constant between the ion and carrier and u_{1s} or u_{2s} is the mobility of the ion-carrier complex; i.e., that the permeability ratio and equilibrium selectivity ratio are nearly the same because all ion-carrier complexes have approximately the same mobility.

To a large extent the forces governing nonequilibrium selectivity are the same as those governing equilibrium selectivity, acting in the opposite direction. However, Born repulsion forces ("steric effects") may assume addi-

tional importance: in sufficiently rigid and close frameworks, steric effects may reduce the mobility of larger ions, giving rise to ion sieving. Two clear and typical examples of the extent of this effect, which should neither be neglected nor overstressed, may be drawn from ion exchange studies on the class of aluminosilicates called zeolites [summarized by Sherry in (5)]. The channels and cavities in the relatively rigid zeolite frameworks are often of atomic dimensions, and their sizes can be accurately and independently determined by crystallographic methods for comparison with their experimentally observed sieving properties.

1. The channels in basic sodalite have a free radius of 1.3 Å. The following monovalent ions, all of which have ionic (nonhydrated) radii comparable to or less than 1.3 Å, are found to exchange rapidly (but with different equilibrium affinities) into and out of basic sodalite cages: Li^+ (Pauling crystal radius 0.60 Å), Na^+ (0.95 Å), Ag^+ (1.26 Å), K^+ (1.33 Å). The following ions with larger crystal radii exchange with great difficulty into and out of basic sodalite cages: NH_4^+ (1.40 Å), Tl^+ (1.40 Å), Rb^+ (1.48 Å), Cs^+ (1.69 Å). The *hydrated* radii estimated from a modified form of Stokes' law are about 3.3 Å for Na^+ and 3.7 Å for Li^+ (76, p. 126), i.e. much greater than the basic sodalite channel. The good exchangeability of these ions with small ionic radii but large hydrated radii shows that water of hydration has been readily stripped off these monovalent cations, and that sieving of alkali cations is primarily related to nonhydrated size.

2. Free energies of hydration for divalent cations such as the alkaline earths, and trivalent cations such as La^{+++}, are about 3 to 6 times those of the monovalent alkali cations, respectively. When a polyvalent cation has an ionic radius less than the channel radius but a hydrated radius greater than the channel radius, the cation may be unable to enter the channel, unlike the just-cited result for monovalent cations. For instance, Tl^+ (ionic radius 1.40 Å) diffuses into the sodalite cages of Linde X at 25° C, whereas Ba^{++} (ionic radius 1.35 Å) does not, despite its smaller ionic size. Again, the ionic radius of La^{+++} (1.15 Å) is significantly less than the radius of the sodalite channels in Linde Y (1.25 Å); La^{+++} exchanges completely at 100° C but not at all at 25° C. The hydration energy of these polyvalent cations is evidently too large, and the sodalite framework too rigid, to permit enough stripping of water of hydration and enough vibrational fluctuation in channel size for passage through the sodalite channels to occur at room temperature.

Nonequilibrium steric effects with the strongly hydrated polyvalent cations presumably explain why the glass electrodes are much less permeable to Ca^{++} than to the alkali cations, despite high binding constants for Ca^{++}. For example, the mineral montmorillonite binds Ca^{++} twice as strongly as Na^+, but montomorillonite membranes are 40 times more permeable to Na^+ than to Ca^{++}, because the mobility of Ca^{++} is 80 times lower than that of Na^+ (6). It seems likely that low mobility may similarly explain the low permeability of most biological membranes to Ca^{++}, despite the high equilibrium affinity for Ca^{++} suggested by the ability of small concentrations of

Ca^{++} to suppress permeability of monovalent cations present in much higher concentrations (e.g., 16).

For the alkali cations, however, the available experience indicates that steric effects will be much more closely related to the nonhydrated sizes than to apparent hydrated sizes. Since the "equivalent pore radii" measured for nerve, erythrocyte, and other biological membranes are about 4 to 6 Å (77) and since the largest alkali cation, Cs^+, has a radius of only 1.69 Å, ion-sieving effects in permeation of alkali cations through biological membranes are probably of only secondary importance.

Pore Radius and Alkali-Cation Selectivity

As the final topic in ion selectivity, mention must now be made of attempts to explain all of alkali-cation selectivity in terms of sieving of naked or hydrated ions, attempts which should be of purely historical interest but which are unfortunately still invoked in much current physiological literature.

The experimental facts that have often led physiologists to attribute selectivity to ion sieving and pore radius are that most cells are more permeable to K^+ than to Na^+, K^+ having the smaller apparent (e.g., Stokes' law) hydrated size; and that some biological specificity sequences for cations or anions happen to be in the order of the apparent hydrated sizes (the lyotropic series) or else of the measured nonhydrated sizes. This point of view is similar to that adopted by physical chemists before about 1920. Physiologists still adopting this point of view have apparently not been aware of the large and detailed body of information on ion selectivity, summarized in the preceding pages, that had already necessitated the abandonment of this interpretation by Jenny in 1927: that these two kinds of sequences which do apparently correlate with size are only two out of a class of observed sequences, the others of which correlate neither with nonhydrated nor with apparent hydrated size; that the transitions between these sequences can be produced experimentally by changes in electrostatic forces in nonliving systems, biological colloids, and at least one biological membrane (the gallbladder); that calculations of electrostatic forces correctly reconstruct these sequences; and that the sieving effects on alkali cations demonstrable in narrow-pore systems are primarily related to ionic size. The apparent correlation of the lyotropic series with calculated hydrated sizes is now recognized by physical chemists concerned with ion selectivity to be "a misleading accident" (4, p. 269), since hydration affects ion selectivity through energy balance and not through size considerations: if ion:membrane interactions are energetically weak, they are outweighed by ion:water interactions, and the ion with the lowest hydration energy experiences the largest free energy decrease (or smallest increase) on passing from water to the membrane, yielding the lyotropic series.

The same general objections plus further specific objections are relevant

to two recent misapplications of pore and sieving concepts to ion selectivity. First, some authors (e.g., 78, 79), working with the ion-selective cyclic antibiotics, initially interpreted their selectivity in terms of the ring size of the antibiotic sterically determining the size of the permeating ion (e.g., the hole in the antibiotic's ring might provide a pore through which only certain ions would fit). However, evaluation of the accumulated evidence from macrocyclic compounds of varying ring size shows that there is no simple relation between the ring size and the observed selectivity patterns, which are the same as those observed in other biological and nonbiological systems and predicted from the Coulomb model.

Second, Mullins (74) has argued that a pore might select a partially hydrated ion, with a certain number of hydration shells, of an optimal size and might discriminate against both larger and smaller ions:

> If an ion at a specified level of hydration closely approximates the size and shape of a pore, it may exchange all its hydration, beyond the specified level, for the solvation afforded by the walls of the membrane pore. . . . If K^+ approaches a pore that is precisely the same size as this ion with its first hydration shell (denoted $(K^+)_1$), it may, as indicated previously, exchange hydration, for water shells from 2 to infinity, for *a similar attraction* with the structure lining the pore. If the pore is somewhat smaller than $(K^+)_1$, penetration cannot occur for steric reasons, while if the pore is somewhat too large, penetration likewise cannot occur because the attraction of the ion for water shells of 2 and greater is not compensated by a solvation of *similar magnitude* in the pore.

[(74, pp. 125–126); italics added by the reviewers]. The erroneous assumption implicit in the italicized expressions "similar attraction" and "similar magnitude" is that any nearest neighbor at a given distance, whether water or membrane substance, will exert similar attractive forces upon the ion. In fact, the attractive force exerted by the membrane may be much more or much less than that exerted by water, depending upon whether its field strength is much more or much less than that of water, and it is this variation in electrostatic forces which determines selectivity. In addition, one of the earliest reasons why physical chemists (e.g., 80) discarded Gregor's selectivity theory and Ling's 1952 theory, which were founded on the concept of hydrated size, was the ambiguity of this concept, and Mullins' discussion of the precise fit of a pore to specific hydration shells of an ion is even less defensible physically. Calculated "hydrated ion sizes", whether extracted from Stokes' law, from Debye-Hückel theory, or from other measurements, depend upon what the ion interacts with and what property one is measuring. For instance, the sequence of hydrated sizes obtained from Debye-Hückel theory for Cs^+, Rb^+, and K^+ inverts, depending upon whether F^- (OH^-, acetate) or Cl^- (Br^-,I^-) is the counterion; and the sequence for I^-, Br^-, and Cl^- inverts, depending upon whether Li^+ (Na^+, K^+) or Rb^+ (Cs^+) is the counterion. The use of "hydrated sizes" to explain data other than the data from which they were calculated has virtually dis-

appeared from texts of physical chemistry, since hydration effects can be consistently explained only if the fundamental criterion is energy (as in Eisenman's theory), not size.

Summary of Ion Selectivity

The problem of Na^+-K^+ discrimination by biological membranes is part of the general problem of discrimination among the five alkali cations (Li^+, Na^+, K^+, Rb^+, Cs^+). Although these five ions can be permuted 120 different ways, only 11 of these permutations are consistently observed as selectivity sequences in nonliving systems such as minerals, ion exchange resins, and glass electrodes. It is a striking fact that the selectivity orders observed in most biological systems fit the same pattern of 11 sequences, which suggests that the physical basis of discrimination is the same in nonliving and in living systems. The principal factor controlling cation equilibrium specificity is the field strength of membrane negative charges. A simplified model which estimates the energies of ion:site interaction thermochemically or by Coulomb's law and compares these with free energies of hydration correctly predicts the observed pattern of 11 sequences. The selectivity patterns for halide anions and for divalent cations are constructed; these are also successfully predicted by a Coulomb model. Predictions, which have received some experimental confirmation, can be made relating the expected ion selectivity pattern to the pK_a of the membrane sites with which the ions interact. The contributions to ion selectivity from non-Coulomb forces, hydration, site spacing, entropy effects, and nonequilibrium effects such as ion sieving are summarized.

PART II. NONELECTROLYTE SELECTIVITY

Introduction

If one makes a comparison of pairs of nonelectrolytes with approximately the same sizes, molecular weights, free-solution diffusion coefficients, and empirical formulae, one finds that permeability coefficients measured in the same biological membrane may differ by a factor of up to 10^8 between members of a pair. This selectivity is of interest not only because of its physiological importance, but also because it arises directly from the structure of much of the cell membrane and thus provides evidence concerning membrane structure.

Nonelectrolytes vary enormously in size, shape, structure, intramolecular interactions between substituent groups, and interactions with other molecules, as well as in permeating power. Thus, studies which attempt to draw conclusions about the general patterns of selectivity but are based on permeability determinations for a few molecules run the risk of yielding misleading results, although such studies may be useful in the further analysis of specific problems once the general patterns have been established. Most of the discussion will therefore center on two comprehensive investigations of nonelectrolyte permeation: the studies of Collander (81–96) on giant algal

cells of the family Characeae and on model systems; and the permeability determinations by Wright & Diamond (97–99) in rabbit gallbladder epithelium. Fortunately, although no two biological objects could be more dissimilar than giant algae and rabbit gallbladders, the qualitative patterns that emerge from these two studies are in detailed agreement, and studies on other tissues appear to provide merely quantitative variants of these same patterns. We shall begin by describing the algal and gallbladder experiments and presenting the permeability patterns that were obtained. It will be shown that the main pattern of nonelectrolyte selectivity is similar to that in simple model systems, and that the three classes of deviations from this main pattern are related to the specific structure of biological membranes. Finally, the origin of main-pattern selectivity will be discussed on the basis, first, of a thermodynamic analysis using incremental partial molar quantities associated with specific residues, and then on the basis of intermolecular forces. Discussion will be confined to selectivity associated with passive, noncarrier-mediated permeation, since the nonelectrolyte selectivity patterns associated with permeases and active transport mechanisms are quite different, in contrast to the situation for ions.

Giant Algae and Rabbit Gallbladders

The Characeae or stoneworts are a family of green algae whose cells may be up to several inches long, 1 mm or more thick, and nearly cylindrical in shape. Most of the volume of the cell is the vacuole, separated by a typical plasma membrane (the tonoplast) from a layer of protoplasm, which is separated in turn by another typical plasma membrane (the plasmalemma) from an external cellulose wall up to 10 μ thick. The most extensive quantitative study of permeation in the Characeae was Collander's determination of permeability coefficients for 70 nonelectrolytes in cells of the alga *Nitella mucronata* by direct chemical analysis (81). In most cases the efflux rate of a substance from a cell which had previously equilibrated with a solution of the substance was measured, while influx rates were determined for the least permeable substances. Numerous different nonelectrolytes were often compared directly on the same cell. Collander measured the permeability of heat-killed cells and subtracted the resulting resistance (the reciprocal of the permeability coefficient) from the resistance of the live cell to obtain a resistance corrected approximately for unstirred layers. A similar, earlier study (82) by Collander & Bärlund yielded permeability coefficients for 45 nonelectrolytes in the related alga *Chara ceratophylla*. In scope, care, and value these two studies offer by far the best measurements of permeability coefficients to date.

Some other studies by Collander which are of equal importance and quality but which have unfortunately tended to be overlooked by animal physiologists deserve to have specific attention drawn to them here: permeability to rapidly penetrating nonelectrolytes, measured by an osmotic method (83); permeability to small molecules (84, 85); permeability to

branched molecules (86); permeability to very large molecules (87); permeability of other plant, fungal, bacterial, and yeast cells (88–91); partition between bulk lipid solvents and water (92–95); the chemical interpretation of partition phenomena (95); and a general review of nonelectrolyte permeation and partition phenomena by Wartiovaara & Collander (96).

Rabbit gallbladder is a sac consisting of a single layer of uninterrupted epithelial cells fused to each other around the whole circumference by continuous tight junctions, and supported on the outside by connective tissue. Wright & Diamond (97–99) measured the permeability of this epithelium to 206 nonelectrolytes. The parameter determined was not the permeability coefficient but the reflection coefficient or Staverman coefficient σ (100), which is the ratio of the osmotic flow caused by a gradient of a test molecule to the flow caused by the same gradient of a molecule known to be impermeant. This ratio is 1 for an impermeant molecule and decreases progressively below 1 for increasingly permeant molecules until $\sigma = 0$ is reached for a solute as permeant as water. This relation between osmotic flow rates (effective "osmotic pressure") and the permeability of the solute responsible for the osmotic gradient is due to two facts: the osmotic flow rate from dilute to concentrated solution is reduced below the volume flow rate of solvent in this direction by the volume flow rate of solute diffusing down its concentration gradient from concentrated to dilute solution; and the diffusing solute may drag some solvent from concentrated to dilute solution, if and only if solute and solvent interact while crossing the membrane. Thus, the following expression holds (101):

$$\sigma = 1 - \omega v_s / L_p - K f_{sw} / (f_{sw} + f_{sm}) \qquad 2.$$

where ω is the solute permeability coefficient and v_s its partial molar volume, L_p is the hydraulic conductivity, K a partition coefficient, and the f's are frictional coefficients between solute and water (f_{sw}) or solute and membrane (f_{sm}). In addition, measured σ's for permeant molecules are reduced still further below 1 in proportion to their permeability, as a result of dissipation of the solute concentration gradient in unstirred layers adjacent to the membrane.

Flow rates can be measured in rabbit gallbladder in a fraction of a minute by means of streaming potentials, so that in practice Wright & Diamond took σ as the ratio of the streaming potential produced by 0.1 molal of the test substance to the streaming potential, measured immediately before and afterwards, produced by 0.1 molal of the impermeant solute sucrose. Smyth & Wright (102) had previously found close agreement in the intestine between σ's measured by this electrical method and σ's obtained from a gravimetric procedure for measuring flow rates, as expected from the observed direct proportionality between streaming potentials and flow rates (103); and Collander had previously found that a similar osmotic procedure yielded virtually the same permeability sequences in *Nitella mucronata* as did direct chemical analysis (81, 83). The advantages resulting from the rapidity of

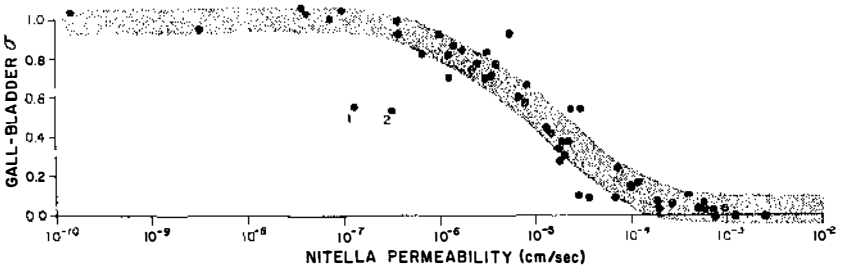

FIG. 3. Ordinate, reflection coefficients (σ's) of nonelectrolytes measured in rabbit gallbladder epithelium by Wright & Diamond (98). Abscissa, permeability coefficients of the same nonelectrolytes measured in the alga *Nitella mucronata* by Collander (81). The two deviant points are urea (1) and methyl urea (2). Except for these two solutes, gallbladder σ's decrease closely in parallel with increasing permeability in *Nitella*, showing that the two systems have essentially the same permeability pattern. The shaded band is drawn to indicate the general trend of the points and has no theoretical significance.

this electrical method were that several dozen σ's could be determined in a single experiment, facilitating comparison of closely similar molecules in the same preparation; and that σ's could be obtained for unstable molecules which undergo rapid chemical transformation on being dissolved in water and which therefore yield erroneous permeability values by slower methods. Of the three papers reporting these experiments, the first (97) presented the method, the second (98) analyzed the patterns of permeation and the effects of pH and temperature, and the third (99) analyzed the molecular forces responsible for nonelectrolyte selectivity.

Figure 3 plots σ's in the gallbladder against P's or permeability coefficients ($P=\omega RT$) in *Nitella mucronata* for 52 solutes of varying sizes, shapes, and solubility properties studied in both preparations. Except for urea and methylurea, the results correlate closely: gallbladder σ's decrease from 1 to 0 with increasing permeability in *Nitella mucronata*. Two conclusions follow from this correlation: that in either preparation σ's measured by streaming potentials would be closely correlated with permeability coefficients measured by direct chemical analysis; and that nonelectrolyte permeation is governed by the same selectivity principles in rabbit gallbladder epithelium as in the alga *Nitella mucronata*.

Three general questions concerning active transport, complex membranes, and unstirred layers apply to the interpretation of these results or of any other study of nonelectrolyte permeation. First, no mechanism for active transport or facilitated diffusion of a nonelectrolyte has been discovered in *Nitella* or the gallbladder, although the transport properties of both have been the subject of much work; solutes whose transport is carrier-mediated in other tissues (glycerol, sugars, amino acids) show permeability properties in *Nitella* and the gallbladder expected for simple diffusion; and on teleologi-

cal grounds neither preparation would be expected to have active transport mechanisms for nonelectrolytes. The measurements may therefore be safely interpreted in terms of passive permeation. Second, both *Nitella* and the gallbladder are complex membranes, consisting of two membranes in series. The relative resistances of the tonoplast and the plasmalemma to nonelectrolytes in *Nitella mucronata* are unknown. In the gallbladder, it is likely, though not certain, that the electrical method measures σ's for the membranes at the luminal faces of the epithelial cells; but the membranes at the luminal and serosal faces appear in any case to have the same relative permeability properties (97). Finally, measured "membrane resistances" (reciprocals of permeabilities) are the sum of the true cell membrane resistance plus the resistance of adjacent unstirred layers. The more permeant the solute, the greater is therefore the unstirred-layer effect, which causes measured P's and σ's to be lower than real ones. Since the unstirred-layer effect is itself proportional to real permeability, it is of minor importance if one analyzes empirical relations between measured permeabilities and other properties (solubilities, chemical structure, etc.), but is of critical importance when one requires absolute values of σ's or P's or their ratios to insert into kinetic or thermodynamic equations tacitly assuming perfect stirring. The gallbladder results were not corrected for unstirred-layer effects, which may have been considerable for the more permeant solutes. Collander (81) attempted to correct for unstirred-layer effects by measuring and subtracting the resistance of the dead cell; this procedure has not escaped criticism (104, p. 302) but should nevertheless hold approximately, and the correction is in any case significant only for Collander's most permeant solutes. Further discussion of this important unstirred-layer problem will be found in (97, 104–106).

Patterns of Nonelectrolyte Permeability

The main pattern.—Seventy years ago Overton (107) suggested on the basis of extensive but largely qualitative studies that nonelectrolyte permeability correlated well with the lipid solubility of the test solute relative to its water solubility. This concept, which provided the earliest evidence for the key role of lipids in cell membranes, has been quantitatively confirmed by the *Nitella* and gallbladder studies.

If the mechanism of nonelectrolyte permeation were the same through cell membranes as through a bulk lipid phase, the following expression should hold:

$$P_i = K_i D_i / d \qquad 3.$$

where d is the membrane thickness, $P_i = \omega RT$ is the permeability coefficient of the ith solute, D_i is its diffusion coefficient in the membrane interior, and K_i is its lipid:water or membrane:water partition coefficient (the equilibrium ratio of the test solute's concentration in a lipid phase to its concentration in water, the two phases being in contact and mutually immiscible).

The tacit assumption behind this equation is that permeation is limited by diffusion in the membrane interior and not by the two phase-boundary transitions (from water to membrane and from membrane to water). While one would ideally like to have K's for membrane lipids themselves, these are unavailable, but many K's have been measured for other lipid solvents, particularly for ether and olive oil (81, 95). As demonstrated experimentally and discussed by Collander (92, 96), K sequences in different lipid solvents are closely correlated, the quantitative differences in K ratios between different solvents reflecting mainly the balance between their hydrogen-bonding and hydrocarbon portions rather than their specific chemical properties. For diffusion coefficients in bulk solvents the relation $DM^{1/2}$ = constant, where M is the molecular weight, holds approximately for small molecules and $DM^{1/3}$ = constant for very large molecules (108; 109, Figure 3.2). Thus, P and σ should correlate closely with $KM^{-1/2}$ in a homogeneous, bulk, lipid membrane.

Wright & Diamond (98) plotted gallbladder σ's against K_{oil}, K_{ether}, $M^{-1/2}K_{oil}$, and $M^{-1/2}K_{ether}$. All four graphs looked much the same, because K_{ether}'s and K_{oil}'s are closely correlated, and because K varied over a 63,000,000-fold range but M only over a 7-fold range for the molecules graphed, so that the presence or absence of the $M^{-1/2}$ term made little difference. Figure 4 is the graph of σ against $M^{-1/2}K_{ether}$. It is apparent that σ decreases from 1.0 to 0 with increasing $M^{-1/2}K_{ether}$, i.e. that permeability increases in close correlation with increasing partition coefficient for the overwhelming majority of the solutes tested. All the conspicuously deviant points belong to two classes of exceptions: small molecules with low K's, whose σ's are much lower than the main pattern (points 1 through 9, Figure 4); and highly branched molecules, whose σ's are much higher than the main pattern (points 10 through 13, Figure 4).

Collander (81) plotted *Nitella* P's against various functions of M and K_{oil} or K_{ether}. Since M varied over a 25-fold range among the solutes tested, the *Nitella* results are a more sensitive test of the size dependence of permeation than the gallbladder results. P increased conspicuously with increasing K, but also increased somewhat with decreasing M at constant K. Collander concluded that the best empirical fit of P was to $M^{-1.6}(K_{oil})^{1.32}$: the expression $PM^{1.6}/K^{1.32}$ was roughly constant and independent of M above $M = 70$. However, the expression increased progressively with decreasing M below about $M = 70$ (81, Figure 4). Thus, in *Nitella* as in the gallbladder, permeability increases with the partition coefficient, but the smallest molecules are more permeant than expected from the main pattern. Analysis of P's measured by Collander & Bärlund in *Chara ceratophylla* yielded the same conclusion (82).

The pattern of nonelectrolyte permeability may therefore be tentatively summarized as a main pattern with three classes of exceptions: sequences and ratios of permeability coefficients in biological membranes are similar to those for permeation through a bulk lipid phase, except that: the size

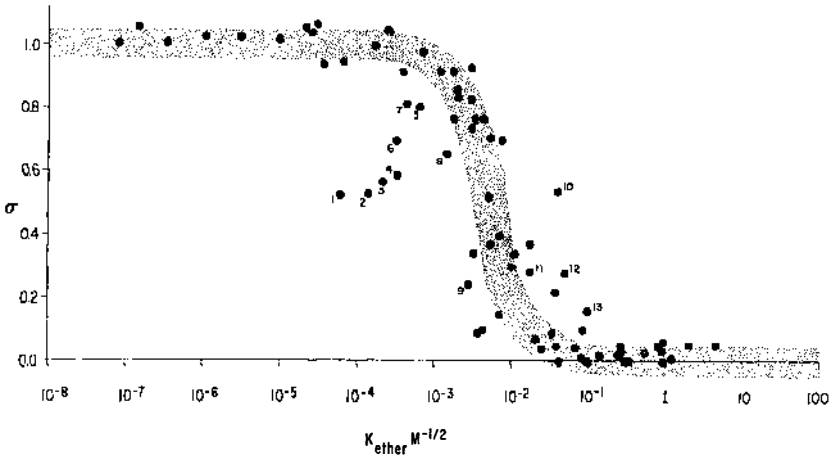

FIG. 4. Ordinate, reflection coefficients (σ's) of nonelectrolytes measured in rabbit gall bladder by Wright & Diamond (98); abscissa, the ether:water partition coefficient (K) times the reciprocal square root of molecular weight (M) for each nonelectrolyte. Points referring to small solutes and branched solutes are numbered: small solutes, 1 = urea, 2 = methyl urea, 3 = formamide, 4 = acetamide, 5 = ethylene glycol, 6 = dimethyl urea, 7 = ethyl urea, 8 = propionamide, 9 = dimethyl formamide; branched solutes, 10 = pinacol, 11 = isovaleramide, 12 = 2-methyl-2,4-pentanediol, 13 = triacetin. The shaded band is drawn to indicate the general pattern of the other points and has no theoretical significance. (From 98.)

dependence is steeper (ca. $M^{-1.5}$ rather than $M^{-0.5}$); small molecules permeate relatively more rapidly; and branched molecules permeate relatively more slowly. Further evidence for the reality of these three exceptions, and discussion of their significance, will be postponed until after discussion of the main pattern.

The significance of the main pattern.—The main pattern (i.e., the close correlation between P's or σ's and K's for most molecules) means that the intermolecular forces governing selective nonelectrolyte permeation through cell membranes are the same as the forces governing nonelectrolyte partition between a bulk lipid phase and water.

This tautology is consistent with either of two different permeation mechanisms: (*i*) The rate-limiting step is diffusion through the membrane interior, as implicit in the equation $P = KD/d$; the achievement of partition equilibrium at the two membrane: water interfaces is very rapid; differences in P's for different solutes are due principally to variation in K's, which is much greater than variation in D's (this is true for bulk solvents); and K's for membrane lipids correlate closely with K's for various bulk lipid solvents, which correlate closely with each other. Two or all of the three observed classes of deviations from the main pattern would find a ready ex-

planation in expected limitations upon the validity of bulk-phase extrapolations to very thin membranes. (*ii*) Diffusion through the membrane interior is relatively rapid, and the rate-limiting step is passage through the water:membrane interface. The activation energy for crossing this interface will be determined by essentially the same intermolecular forces which govern lipid:water partition coefficients, namely, the forces between solute and water which must be broken and the forces between solute and lipids (or membrane) which are gained. Solute:water forces are generally considerably stronger than solute:lipid forces (p. 633) and dominate both partition coefficients and, presumably, activation energies. These two mechanisms represent opposite extremes in a spectrum of possibilities: the resistance of the membrane interior and of the water-to-membrane interface might be comparable, or the balance might differ for different solutes in the same membrane.

The dilemma in clarifying this unresolved problem of the rate-limiting step in permeation is that the governing intermolecular forces and the expected selectivity patterns are the same in either case, so that discussions in terms of one mechanism can be reworded in terms of the other mechanism with equal validity. This ambiguity is illustrated by the fact that Stein (109), who assumed the second mechanism to hold for most molecules, and Diamond & Wright (99), who assumed the first mechanism to hold, invoked essentially the same kinds of chemical arguments and selectivity principles as each other and as Collander (95) had invoked in explaining bulk lipid:water partition coefficients. Three attempts based on the transition-state theory of activated diffusion have been made to resolve this question, but all three appear to us to be invalidated by this equivocal nature of the arguments:

(*a*) The application of activated-diffusion theory to membrane permeation was pioneered by Danielli (110), who assumed that the chief resistance to slowly permeating solutes is at the water-to-membrane interface but is in the membrane interior for rapidly permeating solutes. As Zwolinski et al. (111) point out, this assumption is groundless: the magnitude of the permeability coefficient gives no indication about the locus of the resistance.

(*b*) Zwolinski, Eyring & Reese (111) assumed that the increase in permeability associated with a $-CH_2-$ group (i.e., the increase in P and decrease in σ in a homologous series with increasing hydrocarbon chain length) arose mainly from an increase in K due to a decrease in the rate constant for crossing the membrane-to-solution interface (k_{ms} in their terminology), and that the rate constants for diffusion within the membrane (their k_m) and for crossing the solution-to-membrane interface (their k_{sm}) were little changed. Their tacit assumption was that the $-CH_2-$ group primarily increases solute:lipid forces without changing solute:water forces. On this basis they calculated relative resistance loci for various solutes in various cells. However, it is now clear (pp. 635, 641) that much of the increase in permeability

brought about by a $-CH_2-$ group represents a decrease in solute:water forces due to an entropy effect.

(*c*) Stein (109) has published a valuable analysis of P's measured by Collander and others on the basis of the equations of Zwolinski et al. (111), but tacitly made the same unjustified starting assumption as did Danielli. Reasoning correctly that the water-to-membrane interfacial resistance will depend largely on the number of solute-to-water hydrogen bonds, he extrapolated a graph of log $PM^{1/2}$ against estimated number of hydrogen bonds for various solutes to obtain the limiting maximal $PM^{1/2}$ for a non-hydrogen-bonding solute (109, Figures 3.6 and 3.11). He interpreted the ΔF, ΔH, and ΔS calculated from the slope of this graph as thermodynamic parameters of the transition state for interfacial passage, interpreted the intercept P as the D/d of a non-hydrogen-bonding solute such as a pure hydrocarbon, and thus attempted to estimate diffusion coefficients in the membrane interior. However, one can equally well interpret Stein's ΔF, ΔH, and ΔS as the equilibrium parameters of partition between solute and membrane (cf. Equation 4, p. 630), if one assumes at the opposite extreme [as we have elsewhere (99)] that the membrane interior is rate limiting for most solutes. Stein's assumption that pure hydrocarbons would be limited by the membrane interior is also not necessarily valid because of the same underlying ambiguity: the same arguments which predict low interfacial resistance to a hydrocarbon explain its high partition coefficient (hence low membrane-interior resistance). Finally, even if Stein's assumptions about resistance loci were correct, his intercept would equal KD/d, not D/d, and hence would not yield D without knowledge of K.

The exceptions to the main pattern.—The three respects in which permeation patterns through cell membranes differ from those through a bulk lipid phase provide important clues to the structure of cell membranes.

The effect of branching.—In bulk lipid solvents, branched molecules have lower K's than straight-chain homologues, for reasons discussed on p. 624. However, quantitative comparisons of P's or σ's in several cells with bulk-solvent K's show that cell membranes discriminate even more sharply against branched solutes than does a bulk lipid phase:

(*a*) From the gallbladder results, the most markedly deviant point on the right-hand side of Figure 4 is number 10, pinacol 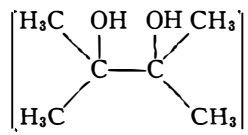 , the only solute tested with two tertiary-carbon branch-points. The main pattern predicts that it should be freely permeant ($\sigma \sim 0$), but its σ is actually 0.54. Three other solutes with too high σ's (too low permeabilities) in Figure 4 each have one tertiary-carbon branch-point: number 11, isovaler-

amide 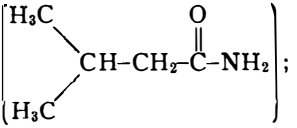 ; number 12, 2-methyl-2,4-pentanediol 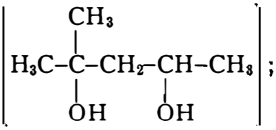 ; and number 13, triacetin 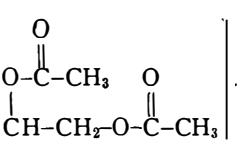 . Comparison of the four isomeric butanols is also instructive (98, Table 3): the branched isobutanol 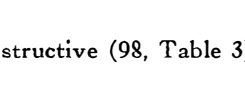 has higher ether and olive oil K's than the straight-chain *sec*-butanol  but is less permeant (has a higher σ); and the most highly branched isomer *tert.*-butanol 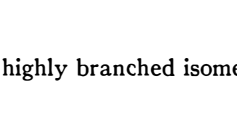 has a much higher σ than the other three isomers, quite out of proportion to the modest difference in K's.

(*b*) In *Nitella mucronata* Collander (81) showed that four solutes with a tertiary-carbon branch-point (*tert.*-butanol, triacetin, trimethyl citrate, and triethyl citrate) had lower P's than expected from the main pattern of *Nitella.*

(*c*) Oura, Suomalainen & Collander (91, Figure 2) showed for three kinds of yeast that the branched isovaleric acid and isobutyric acid were not only less permeant than the straight-chain *n*-valeric acid and *n*-butyric acid but also less permeant than expected from the main pattern in each yeast.

(*d*) Collander (90, Figure 1) indirectly measured permeability of *Elodea* leaves and found that dimethyl malonic acid 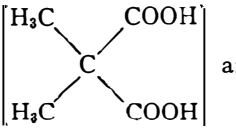 and two acids with tertiary-carbon branch-points (tricarballylic and aconitic acids) were less permeant than expected from the main pattern.

(*e*) Collander (86) showed that the highly branched pentaerythritol 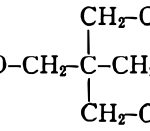 has a higher K_{ether} than the straight-chain erythritol 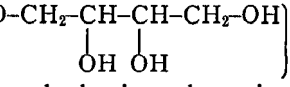 but permeates more slowly in three plant cells and a luminous bacterium.

The fact that cell membranes discriminate more sharply against branched solutes than do bulk lipid solvents is probably attributable (96, 98, 112) to the fact that lipid molecules possess a more highly ordered configuration in cell membranes than in bulk solvents and may even have the hydrocarbon tails of the fatty acid residues aligned in parallel (110). Lipid: lipid forces are largely very short-range van der Waals forces, which are effectively proportional to surface contact area. A branched molecule has less area of close contact with surrounding molecules than does a nonbranched molecule, so that the latter should experience stronger van der Waals forces. This difference will be amplified in an environment where the solvent molecules are rigidly oriented and less free to bend around a solute molecule. The distortion in an oriented solvent structure caused by a branched molecule would also locally reduce the intermolecular forces between the solvent molecules themselves. One therefore expects the enthalpy change for transfer from water to lipid to be less negative, and the lipid-to-water partition coefficient to be lower, for a branched solute, and this difference to be exaggerated in the less flexible molecular arrangement of the membrane interior as compared to the situation in bulk lipid solvents. In addition, membrane lipid structure may act like a molecular sieve in preferentially depressing the diffusion coefficient of a branched solute relative to free solution.

The effect of size.—To determine the effect of size per se as distinct from other molecular properties requires permeability determinations for a very large number of solutes covering a wide range of molecular weights, since size effects are otherwise obscured by the huge range (10^8-fold) in K's among nonelectrolytes. The only adequate test is provided by the *Nitella* results, where Collander initially (81) concluded that P varied as $M^{-1.5}$ between molecular weights $M=70$ and $M=480$. Later (87) Collander tested two polypropylene glycols with $M=425$ and $M=1025$ and obtained lower permeabilities than predicted from an $M^{-1.5}$ dependence. On recalculation we find that a dependence between $M^{-2.5}$ and M^{-3} is required to explain the polypropylene glycol results and is compatible with the earlier *Nitella* results. This inverse dependence on size is far steeper than the $M^{-1/2}$ or $M^{-1/3}$ dependence observed for diffusion in free solution, and may have the same explanation as the discrimination against branched molecules: the distortion introduced by a large solute molecule into the oriented hydrocarbon in-

terior of a membrane would reduce the solute's partition coefficient, and might also reduce its diffusion coefficient because of a molecular-sieve effect.

Permeation of the smallest solutes.—In *Chara ceratophylla* (82) and *Nitella mucronata* (81) the smallest solutes (water, methanol, formamide, acetamide, etc.) permeate more rapidly than expected from the main pattern. In the gallbladder all solutes tested that are both small ($M < 75$) and have low partition coefficients ($K_{ether} < 0.1$, $K_{oil} < 0.007$) have σ's far below the main pattern (points 1 through 9, Figure 4). Most of these deviant small solutes are relatively polar molecules (ureas or amides). For example, urea (point 1, Figure 4) should be impermeant ($\sigma = 1.0$) according to the main pattern but actually has $\sigma = 0.53$, a value expected only for a molecule 100 times more lipid-soluble than urea actually is. These deviations persist even if the size dependence of the main pattern is taken as M^{-3} or M^{-4}. It is possible that nonzero values of the water-drag component of σ, $Kf_{sw}/(f_{sw}+f_{sm})$ in Equation 2 (p. 616), contribute to these low σ's in the gallbladder, but it seems safe to assume that in addition permeability is much higher than normal, by analogy with the *Nitella-Chara* results in which P's rather than σ's were measured.

Two possible explanations for the anomalously high permeability of the smallest and most polar solutes must be considered: First, these solutes may follow the same route through membrane lipids as do other solutes, and their enhanced permeation may be another expression of the sieve properties of oriented membrane lipids. Detailed statements of this interpretation have been presented [Wartiovaara (112), Wartiovaara & Collander (96)]. Second, these solutes may follow a separate route through the cell membrane, interacting with membrane polar groups rather than with the hydrocarbon tails of lipids. The latter interpretation, according to which the membrane behaves as a mosaic towards permeating solutes, appears to us more probable for the following five reasons:

(*a*) For molecules fitting the main pattern of permeation, the relations between chemical structure and permeability are summarized in a set of rules which were first formulated empirically by Overton, which also apply to lipid:water partition coefficients, and which are readily explained in terms of differences between solute:water forces and solute:lipid forces. However, there are many instances in the gallbladder and other tissues where a change in structure of a small molecule produces a change in permeability that violates Overton's rules and is apparently related primarily to size. Typical examples are the cases in which the second compound in a homologous series is less permeant than the first, although the addition of each subsequent $-CH_2-$ group increases permeability [e.g., the order of σ's in the gallbladder is formamide < acetamide > propionamide > butyramide > valeramide > hexanamide, and methanol < ethanol > propanol > butanol; the order of P's in mitochondria (113) is formamide > acetamide = propionamide < butyramide < valeramide. See (98, Tables 4 and 5) for many other examples.] Correspondly, the magnitude of the deviation of gallbladder σ's of

small solutes from the main pattern shows no correlation with partition coefficients or Overton's rules. This suggests that these solutes interact with hydrocarbon tails of membrane lipids minimally or not at all.

(*b*) If the explanation were the same sieving effect in the lipid phase responsible for $M^{-1.6}$ dependence, one might expect this effect to restrict permeation continuously and increasingly from the smallest to the largest solute. In fact, both in *Nitella* and in the gallbladder a single empirical relation describes P's or σ's of all solutes above about $M = 70$ to 90 and the enhanced permeation of polar solutes appears only below this size. The *Nitella* results, incidentally, suggest that the "extra" permeability of water is simply that expected from extrapolation of the "extra" permeability of other small solutes to the size of the water molecule (81, Figure 4).

(*c*) In the gallbladder, σ's for solutes fitting the main pattern increase markedly at low pH, possibly because of altered charge and packing of membrane lipids. On the other hand, σ's for the deviant small solutes remain virtually unchanged (98, Table 9), again suggesting that they bypass membrane lipids. The same interpretation may underlie the observation in toad urinary bladder (114) that permeabilities to non-ionic forms of fatty acids decrease at low pH, the effect becoming more marked with increasing chain length (increasing lipid solubility) (see 98 for further discussion).

(*d*) In the gallbladder, σ's for solutes fitting the main pattern decrease greatly with increasing temperature, while the effect of temperature is much less marked on σ's of the deviant small solutes (98, Tables 6, 7, and 8). This means that the temperature coefficient of permeation is higher in the lipid pathway than in the polar pathway, perhaps because more energy is required for solute transfer from water to lipid than from water to another polar environment. Wright & Diamond (98) showed that the formerly confusing patterns obtained by Wartiovaara (115–117) for Q_{10}'s of nonelectrolyte permeation in six kinds of plants can be easily rationalized if there is a separate polar pathway with low Q_{10}'s. Even if one considers only those solutes fitting the main pattern and following the lipid route, Danielli's prediction that "$PM^{1/2}$ and (Q_{10}) are negatively correlated for a homogeneous membrane" (110, p. 332) is unlikely to be confirmed. This prediction would be valid only if ΔF for permeation or partition could be equated with ΔH and if entropy changes were negligible. In fact, entropies of permeation are large (109, 111) and in many cases (pp. 635, 641) outweigh enthalpies.

(*e*) Sequences of permeation rates of larger nonelectrolytes are very similar in different cells, but sequences involving smaller nonelectrolytes show much variation. For instance, a survey of erythrocytes of 39 vertebrate species by Jacobs, Glassman & Parpart (118) revealed that 22 were more permeable to thiourea than to urea, 17 vice versa; Höber & Ørskov (119) surveyed erythrocytes of nine vertebrate species and found urea more permeant than methylurea in five species, vice versa in four, and acetamide more permeant than propionamide in four species, vice versa in four, equally

permeant in one; Collander & Wikström (85) studied protoplasts of 36 plants and found 31 more permeable to methylurea than to urea, vice versa in five. There is a voluminous literature, particularly by botanists, on these reversals, which have been used to define "permeability types" ("urea-permeable," "methylurea-permeable") and for which diverse explanations specific to particular molecules have been advanced. Most of this variation between different tissues, different species, or different individuals is of the kind one would expect if there were separate lipid and polar pathways whose relative contributions to nonelectrolyte permeation varied in different cases, and if in addition the upper size limit for permeating solutes in the polar pathway varied.

The following two cases suggest variation in the lipid pathway with little variation in the polar pathway: (*i*) σ's for four nonelectrolytes were measured in axons of the Chilean squid *Dosidicus gigas* (120) and the Venezuelan squid *Doryteuthis plei* (121). Values for the two least lipid-soluble solutes, urea and glycerol, showed little species difference, but σ's for the more lipid-soluble formamide and ethylene glycol were much lower in *Dosidicus* than in *Doryteuthis*. (*ii*) In *Doryteuthis* σ's decrease during electrical stimulation. This decrease is marked for the solutes with the highest K's and is slight for the solutes with the lowest K's (121, Table 3 and Figure 5), which suggests some reorganization of membrane lipids during the action potential.

The following three cases imply variation in the polar pathway with little variation in the lipid pathway: (*i*) Collander (81) found two *Nitella mucronata* cells which were up to three times more permeable to small polar solutes than most other cells but whose permeabilities to larger solutes with higher K's were normal. (*ii*) The bacterium *Beggiatoa mirabilis* became a frequently cited extreme case on the basis of Ruhland's & Hoffmann's claim (122) that permeability was correlated solely with size and not at all with lipid:water K's. Examination of Schönfelder's more detailed study (123) shows that P does increase with K at constant M, and that *Beggiatoa* is unusual only in that the polar route passes molecules up to the size of disaccharides (diameters ca. 10 Å), rather than cutting off around 3-carbon compounds (diameters ca. 5 or 6 Å), as in *Nitella* and the gallbladder. Some diatoms behave similarly to *Beggiatoa* in this respect (88). (*iii*) The opposite extreme from *Beggiatoa* is the alga *Valonia ventricosa*, which, by several criteria discussed on p. 628, behaves as if it lacked a polar pathway, although its permeability to nonpolar solutes is similar to that of the Characeae. Gutknecht (124) showed that σ's for four small polar solutes in *Valonia* (urea, formamide, acetamide, ethylene glycol) were near 1, and that P for water was so low that σ for methanol was actually negative.

If one accepts this evidence of an additional permeation pathway for small polar solutes, how can it be interpreted in terms of the molecular structure of cell membranes? Whatever polar groups (proteins, or the polar ends of lipid molecules) are present in the membrane interior will interact more

strongly with each other than with hydrocarbon tails of membrane lipids, so that in the most stable configuration these groups would be aggregated into polar regions instead of being dispersed among the hydrocarbon tails. Associated with the polar groups will be water molecules in a more or less "frozen" state, as in crystalline hydrates. These polar regions may be few, as in the Davson-Danielli model, or numerous, as in some more recent membrane models (e.g., 125), and may be permanent or constantly rearranging. Since solute molecules following these polar routes would not contact hydrocarbon tails of membrane lipids or pass out of a polar environment, no correlation between the permeability of these regions and lipid: water K's or Overton's rules is expected, and steric factors in the polar framework would set an upper limit to the size of permeating solutes. The total permeability to a given solute would be the sum of its permeabilities in the two pathways.

The polar route is also probably responsible for several other distinctive permeability properties which are present in most (but not all: cf. *Valonia*) cell membranes and absent in membranes composed purely of lipids: (*a*) There has been a long debate over whether the osmotic permeability to water P_f is greater than the diffusional permeability P_d, with much of the earlier evidence invalidated by neglect of unstirred-layer effects. Careful recent studies by Sha'afi et al. (126), Gutknecht (124), Finkelstein & Cass (56), and Dainty & House (105) show conclusively that P_f is greater than P_d in erythrocytes and probably in frog skin but that P_f equals P_d in the alga *Valonia* and in artificial membranes of pure lipids. $P_f > P_d$ implies interactions (e.g., frictional) between permeating water molecules as would arise in a polar route, while $P_f = P_d$ implies singly diffusing, noninteracting water molecules, as expected and found in the thin lipid membranes. (*b*) Solvent-drag effects of water on permeating small nonelectrolytes have been demonstrated in frog skin (127) but are absent in *Valonia* (124). As implied by electrokinetic phenomena, drag effects between water and permeating ions have been demonstrated in the algae *Chara australis* and *Chaetomorpha darwinii* by Barry (128) and in squid axon by Vargas (120). (*c*) As implied by values of σ less than $1-\omega v_s/L_p$ (see Equation 2, p. 616), drag effects of permeating solutes on water exist in erythrocytes (129) and in *Nitella* (130) but are absent in *Valonia* (124). The inference that high permeability to water and small polar solutes is correlated with $P_f > P_d$, solvent drag, electrokinetic phenomena, and solute drag, and that all these effects arise at the same membrane structures, which are distinct from hydrocarbon tails of membrane lipids, is supported by the fact that none of these phenomena has been demonstrated in thin lipid membranes or in the alga *Valonia*, but that some or all have been demonstrated in erythrocytes, frog skin, squid axon, gallbladder, intestine, and the Characeae.

In regard to the upper size limit for solutes using the polar route, equations derived from macroscopic sieving theory have been applied to σ's and P's by Solomon (77) and others and used to calculate "equivalent pore

radii" for biological membranes. The appropriate parameters to use in such calculations are not σ's and P's themselves, but instead the deviations of σ's and P's from the main pattern, i.e. the permeability associated with the polar route alone. Most published calculations of this type have assumed without proof that the solutes in question are "lipid-insoluble" and permeate only via pores, not via lipid. Actually there is no small solute, not even urea, with a K so low that this assumption would in general be justified, since permeation of any given one of the small solutes commonly used for pore-radius determinations occurs primarily through lipid in some cells and primarily via the polar route in other cells. Thus, either the separate determination of σ and P and use of Equation 2, or else the measurement of enough σ's or P's to reconstruct the main pattern in the particular cell under study, would be a desirable adjunct of pore-radius determinations. Deviations from the basic assumption of macroscopic sieving theory, that an object's passage is determined solely by its geometrical properties, are inevitable for nonelectrolytes in molecular-sized pores because of the same types of membrane:solute interaction that control ion selectivity. For instance, among the amino acids histidine, phenylalanine, alanine, and glycine Eisenman found that glass electrodes exhibited five different selectivity sequences which were correlated with field strength and interpretable in terms of solute polarization by charged groups of the glass (13). The biological colloids which Bungenberg de Jong studied for alkali-cation, halide-anion, and alkaline-earth selectivity also yielded examples of selectivity patterns among organic acids, amines, esters, and alkaloids (28). In the gallbladder there are at least four cases or groups of cases in which the deviations of measured σ's of small polar solutes from the main pattern are not explicable on the basis of size, presumably because of these inevitable membrane:solute interactions (98).

The Molecular Basis of Main-Pattern Selectivity

The correlations ("Overton's rules") between molecular structure and permeating power for solutes fitting the main pattern are the same as those describing partition coefficients between a bulk lipid solvent and water. The origin of these selectivity principles lies in the differences between water:nonelectrolyte and lipid:nonelectrolyte intermolecular forces. In the remainder of this chapter we shall analyze these forces from two points of view. First, we shall adopt a thermodynamic approach and calculate the changes which the principal substituent groups produce in the partial molar free energies (and, where possible, enthalpies and entropies separately) of interaction between nonelectrolytes and either water or lipids. These incremental thermodynamic quantities indicate to what extent the nonelectrolyte selectivity of a given membrane is due to differences between various solutes in their solute:water forces, and to what extent it is due to differences in solute:membrane forces. The separation of enthalpy and entropy contributions is also instructive. The conclusions which follow from this thermo-

dynamic analysis are summarized on pp. 633–35. Secondly, we shall attempt to identify what the controlling intermolecular forces actually are.

Incremental thermodynamic quantities.—The following expression relates lipid:water partition coefficients (K's) to thermodynamic properties:

$$K = e^{-\Delta F_{w\to l}/RT} = e^{-(\Delta H_{w\to l} - T\Delta S_{w\to l})/RT} \qquad 4.$$

where $\Delta F_{w\to l}$ is the free energy change in transferring 1 mole of solute from water to lipid solvent (or cell membrane), $\Delta H_{w\to l}$ and $\Delta S_{w\to l}$ are the corresponding partial molar enthalpy and entropy changes, R is the gas constant, and T the absolute temperature ($RT = 592$ cal/mole at 25° C). If nonelectrolyte permeation through cell membranes is limited by diffusion through the membrane interior so that $P = KD/d$ (Equation 3) holds, Equation 4 reads: $Pd/D = e^{-\Delta F_{w\to l}/RT}$. Assuming that variation in P's is due largely to variation in K's and not to variation in D's,[5] one may substitute into Equation 4 the ratio of the permeability coefficients for two solutes differing in a single functional group and obtain the incremental quantities $\delta\Delta F_{w\to l}$, $\delta\Delta H_{w\to l}$, and $\delta\Delta S_{w\to l}$ by which the group alters the partition equilibrium between membrane lipids and water. If nonelectrolyte permeation is limited by the membrane:water interface, these incremental quantities have the significance of activation parameters for the transition state, as assumed by Stein (109). As already discussed (pp. 621–22), present evidence is inadequate to decide which of these interpretations of the parameters of Equation 4 is correct.

Values of $\delta\Delta F_{w\to l}$ associated with various substituent groups (e.g., –OH, $-NH_2$) for transfer from water to isobutanol, water to ether, water to olive oil, or water to *Nitella mucronata* membrane were calculated as follows. Tables of partition coefficients show that in a given solvent system introduction of a given substituent group into a variety of molecules reduces all their K's by a roughly constant factor, characteristic for that particular substituent group and solvent system. The same is true for effects of substituent groups on P's in biological membranes. For instance, an –OH group on the average reduces values of $K_{\text{isobutanol}}$ by 5 times, K_{ether} by 32 times, K_{oil} by 110 times, and P's in *Nitella mucronata* by 450 times. The K or P ratio is substituted into Equation 4 to yield $\delta\Delta F_{w\to l}$ for the given group. To obtain the necessary K or P ratios, we used values of $K_{\text{isobutanol}}$ from (93), K_{ether} from (95), K_{oil} from (81), and P's in *Nitella mucronata* (81), for pairs of compounds differing in the presence or absence of a single substituent group. Thus, in *Nitella*, P is 177×10^{-7} cm/sec for $CH_2(OH)\cdot CH_2\cdot CH_2\cdot CH_2\cdot CH_2\cdot CH_2OH$, 0.42×10^{-7} cm/sec for $CH_2(OH)\cdot CH(OH)\cdot CH_2\cdot CH_2\cdot CH_2\cdot CH_2OH$,

[5] This assumption seems reasonable because at constant molecular weight, K's for a given solvent vary over a 10^{10}-fold range but D's vary over less than a 2-fold range; and because substituents such as $-CH_2-$ groups and halogens, which are known to increase lipid:solute intermolecular forces and to increase K's and presumably to decrease D's slightly, are observed to increase rather than to decrease permeating power.

so that the additional –OH reduces P by $177/0.42 = 420$ times in this case. We also utilized pairs of compounds differing in that an –OH on one was replaced by some other group on another, and obtained $\delta\Delta F_{w\to l}(X)$ by adding $\delta\Delta F_{w\to l}(OH)$ to $\delta\Delta F_{w\to l}(X\text{-}OH)$. For example, K_{ether} is 7.7 for $CH_3\cdot CH_2\cdot CH_2\cdot CH_2OH$, 0.058 for $CH_3\cdot CH_2\cdot CH_2\cdot CONH_2$, so $-CONH_2$ reduces K by $7.7/0.058 = 133$ times more than does –OH in this case; but the average reduction in K_{ether} caused by –OH is 32 times; so that the effect of $-CONH_2$ is a reduction by $(133)(32) = 4200$ in this case. P's for small solutes likely to penetrate via the polar route were excluded for consideration. In the cases of

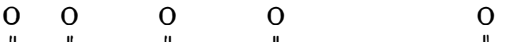

–C–, –C–OH, –C–O–R, –C–NH_2, and –NH–C–NH_2 but not –C≡N the comparisons were chosen so that the introductions occurred by replacement of $-CH_2-$ groups and the total number of carbon atoms in the molecule remained unchanged. Table I lists the average values of $\delta\Delta F_{w\to l}$ obtained in this manner.

To resolve $\delta\Delta F_{w\to l}$ into components associated with solute:water and with solute:lipid interactions, let us imagine that transfer from water to lipid solvent (or membrane) is broken down into two stages: vaporization of solute from an aqueous solution at infinite dilution into vacuum, followed by condensation and solution of solute from vacuum into lipid solvent. Then one write: $\Delta F_{w\to l} = -\Delta F_w + \Delta F_l$ where ΔF_w and ΔF_l are the partial molar free energy of solution at infinite dilution in water and in lipid solvent, respectively (ΔF's of solution equal ΔF's of vaporization with a negative sign). The incremental quantities associated with individual substituent groups may be written $\delta\Delta F_w$ and $\delta\Delta F_l$. Similarly, $\Delta H_{w\to l}$ or $\Delta S_{w\to l}$ can be equated with the difference between two heats or entropies of solution. At infinite dilution the solute:solute forces in the vapor phase responsible for the nonideal behavior of real gases, and solute:solute forces in the aqueous phase, may be neglected, and ΔF_w is a direct measure of the solute:water intermolecular forces (plus the change in water:water forces caused by intrusion of the solute). Similarly, ΔF_l measures solute:lipid or solute:membrane intermolecular forces. (An alternative cycle would be two-stage transfer of solute from water to lipid via a liquid or solid phase of pure solute. This has the disadvantage that solute:solute forces in the solute phase contribute significantly to the resulting ΔF's of solution, which are no longer a measure solely of solute:water or solute:membrane forces. Thus, comparison of solubilities in water may yield misleading conclusions about solute:water forces: e.g., tertiary butanol is more water-soluble than *n*-butanol because in the former case solute:solute forces are weaker, not because solute:water forces are stronger.)

We have calculated values of $\delta\Delta F_w$ and $\delta\Delta F_l$ for each substituent group as follows: Butler (131, Tables 1 and 2), Frank & Evans (132, Table 4), and Franks (133, Table 1) have given tables of ΔF's of solution or vaporization at infinite dilution in water for 41 simple nonelectrolytes, mostly aliphatic hydrocarbons with a single functional group. Inspection of their results

TABLE I

INCREMENTAL FREE ENERGIES OF SOLUTION (calories/mole)

	$\delta\Delta F_{w\to l}$ ($= -\delta\Delta F_w + \delta\Delta F_l$)				$\delta\Delta F_w$	$\delta\Delta F_l$			
	iso-butanol	ether	olive oil	*Nitella*		iso-butanol	ether	olive oil	*Nitella*
-OH	1000	2100	2800	3600	−7000	−6000	−4900	−4200	−3400
-O-	600	1400	1400	800	−4000	−3400	−2600	−2600	−3200
-C(=O)-	—	2100	2200	2500	−6100	—	−4000	−3900	−3600
-C(=O)-OH	1100	1700	2800	—	−8600	−7500	−6900	−5800	—
-C(=O)-O-R	1200	1200	1400	1400	−5400	−4200	−4200	−4000	−4000
-C(=O)-NH$_2$	1700	4900	4800	6200	—	—	—	—	—
-NH-C(=O)-NH$_2$	1900	5500	5300	7300	—	—	—	—	—
-C≡N	—	1100	—	—	−5800	—	−4700	—	—
-NH$_2$	1100	3500	—	—	−6600	−5500	−3100	—	—
-CH$_2$-	−530	−670	−660	−610	160	−370	−510	−500	−450

The second through fifth columns give for each group listed in the first column the average values of $\delta\Delta F_{w\to l}$, the amount by which the group changes the difference between a nonelectrolyte's partial molar free energy of solution in water and its partial molar free energy of solution in isobutanol, ether, olive oil, or *Nitella* membrane. These $\delta\Delta F_{w\to l}$'s were calculated by substituting into Equation 4 the factor by which the group reduced isobutanol : water, ether : water, or olive oil : water partition coefficients or else permeability coefficients in *Nitella*. Each 1000 cal/mole corresponds to a 5.4-fold reduction in partition or permeability coefficients. The sixth column is $\delta\Delta F_w$, the amount by which the group changes a nonelectrolyte's partial molar free energy of solution (out of vacuum) in water. The amounts in the sixth column were added to the amounts in the second through fifth columns to obtain the $\delta\Delta F_l$'s in the seventh through tenth columns, the amount by which the group changes a nonelectrolyte's partial molar free energy of solution (out of vacuum) in isobutanol, ether, olive oil, or *Nitella* membrane. The more positive the value of $\delta\Delta F_{w\to l}$, the more effective is the group at reducing partition coefficients or permeability coefficients; the more negative the value of $\delta\Delta F_w$ or $\delta\Delta F_l$, the more the group promotes solubility in the given solvent.

shows that the difference $\delta\Delta F_w$ between ΔF_w for a hydrocarbon and ΔF_w for the corresponding monosubstituted hydrocarbon (e.g., $CH_3 \cdot CH_2 \cdot CH_3$ versus $CH_3 \cdot CH_2 \cdot CH_2OH$) is a nearly constant quantity for a given functional group, independent of hydrocarbon chain length. For instance, from Butler (131), ΔF_w is +3090 cal/mole for CH_3OH, +10,080 for CH_4, yielding

$\delta\Delta F_w = 6990$ cal/mole for the alcoholic –OH group; ΔF_w is +3490 for n–C_4H_9OH, +10,460 for n–C_4H_{10}, yielding $\delta\Delta F_w = 6970$ cal/mole for the –OH group. Similarly, inspection of these published ΔF_w's shows that the difference between ΔF_w's for two hydrocarbons with different chain lengths but the same functional group is also a nearly constant quantity independent of functional group. Thus, one can also meaningfully define a $\delta\Delta F_w$ associated with the methylene group $-CH_2-$. Table I gives the average values of $\delta\Delta F_w$ we have extracted in this fashion. For each substituent group this $\delta\Delta F_w$ was then added to the value of $\delta\Delta F_{w\to l} = -\delta\Delta F_w + \delta\Delta F_l$ for each lipid solvent to obtain the values of $\delta\Delta F_l$ listed in Table I.

There are two principal sources of uncertainty in the quantities of Table I. First, although values of $\delta\Delta F_{w\to l}$ are relatively constant, and values of $\delta\Delta F_w$ constant to better than 1 per cent, when calculated from monosubstituted hydrocarbons, there is more scatter in $\delta\Delta F$ values deduced from polyfunctional hydrocarbons because of the so-called secondary effects discussed on pp. 639–40. Secondly, when the power of the molecular weight M describing the size dependence of main-pattern selectivity (see pp. 624–25) is better established, values derived from P's should be corrected on this basis, as Stein (109, Tables 3.5 and 3.6) has tentatively done. Since the changes in K produced by substituents are generally much larger than the changes in M, the correction will generally be small, and it does not apply to $\delta\Delta F$'s estimated from K's.

The following conclusions may be drawn from Table I and these thermodynamic considerations:

1. Values of $\delta\Delta F_{w\to l}$ are positive for all substituents in all four systems (isobutanol:water, ether:water, olive oil:water, *Nitella*:water) except for $-CH_2-$. That is, every substituent was found to reduce permeability and partition coefficients except for $-CH_2-$, which increased them.

2. Virtually every substituent group has a negative value of $\delta\Delta F_l$ or $\delta\Delta F_w$ in all five solvents (water, isobutanol, ether, olive oil, and *Nitella*), i.e., is associated with net attractive intermolecular forces. The sole exception is $-CH_2-$ in water, which has a positive $\delta\Delta F_w$ and actually decreases "water solubility".

3. For every substituent (except $-CH_2-$) and for all four systems the value of $(-\delta\Delta F_w)$ is considerably greater than $(-\delta\Delta F_l)$, as follows necessarily from the previous two conclusions. Expressed pictorially, solute:water forces are much stronger than solute:lipid-solvent (or solute:membrane) forces for nonelectrolyte substituent groups, and the differences in these strong solute:water forces largely swamp the differences among the weaker forces in the lipid phase. In this sense the common tendency to view permeability as controlled by "lipid solubility" represents a basic misinterpretation of the observed fact that permeability correlates with lipid:water partition coefficients. Most substituents decrease permeating power because they increase the energy required to tear the solute loose from water, and despite the fact that they also increase solute:lipid attraction. Thus, explanations

for the qualitative selectivity patterns of biological membranes must be sought largely in terms of the physical chemistry of aqueous solutions. This is the reason why the main-pattern selectivity sequences of biological objects as dissimilar as rabbit gallbladders and giant algae are essentially the same.

4. For $-CH_2-$, $\delta\Delta F_w$ is positive but $\delta\Delta F_l$ is negative, i.e., increasing hydrocarbon chain length causes a solute to be "pushed out of" the aqueous phase as well as to be "pulled into" the membrane or lipid phase.

5. Comparison of Butler's (131) ΔF_w's for branched solutes with ΔF_w's for their straight-chain isomers shows that one branch-point in a carbon chain makes ΔF_w on the average 80 cal/mole more positive, which by substitution in Equation 4 would *increase* K's or P's by 14 per cent. This very small effect is opposite to that actually observed, so that the explanation for the large *decrease* in K's or P's associated with branching must be sought in the lipid or membrane phase. As discussed previously (p. 624), the explanation is that the van der Waals forces experienced in a lipid solvent are smaller for a branched molecule than for a straight-chain isomer.

6. While selectivity patterns qualitatively are largely determined by differences in $\delta\Delta F_w$ between different substituent groups, the quantitative differences between different systems must be due to differences in $\delta\Delta F_l$ for a given group. Of the four "lipid solvents" compared, *Nitella* provides the greatest selectivity, in the sense that it has the largest range (6500 cal/mole) of $(-\delta\Delta F_w+\delta\Delta F_l)$ among substituents other than $-CH_2-$, hence the largest spread in P's or K's. For instance, the ratio of P for methyl acetate to P for glycerol is 780,000 in *Nitella*, while the K ratio in olive oil is only 6100, in ether only 4100, and in isobutanol only 26. This is due to the fact that *Nitella* is the weakest "solvent": it has both the smallest range (800 cal/mole) and the lowest absolute values of $\delta\Delta F_l$'s (for substituents other than $-CH_2-$). The most marked differences among $\delta\Delta F_l$'s in the four lipid solvents involve the isobutanol values (higher than in the other three solvents) and the disproportionately high values for $-OH$ and $-COOH$ in ether (higher than in olive oil or *Nitella*, although ether is comparable to olive oil and *Nitella* in $\delta\Delta F_l$'s for other groups). The molecular basis of these variations in $\delta\Delta F_l$'s is discussed on p. 641.

7. Some resolution of these free energy changes into enthalpy and entropy terms is possible and illuminating. In 20 cases Butler (131) obtained values not only for ΔF_w but also for ΔH_w and ΔS_w, so that incremental heats and entropies of solution in water $\delta\Delta H_w$ and $\delta\Delta S_w$ may be obtained. These values show that the effects of the $-OH$, $-NH_2$, $-\overset{\overset{O}{\|}}{C}-$, $-C(=O)-O-R$, and $-O-\overset{\overset{O}{\|}}{C}-OH$ groups (and by analogy, probably, the $-C\equiv N$ and $-COOH$ groups, for which data necessary to obtain $\delta\Delta H_w$ and $\delta\Delta S_w$ are lacking) in increasing water solubility are enthalpy-controlled. For instance, comparison of $CH_3\cdot CH_3$ and $CH_3.CH_2OH$ yields $\delta\Delta F_w = -6860$ cal/mole, $\delta\Delta H_w = -8450$ cal/

mole, $\delta\Delta S_w = -5.4$ cal/mole/degree, $T\delta\Delta S_w = -1610$ cal/mole for the –OH group, which promotes water solubility ($\delta\Delta F_w < 0$) because of the enthalpy term ($\delta\Delta H_w < 0$) and despite the entropy term ($\delta\Delta S_w < 0$). One can describe this result by saying that –OH and most other substituents increase water solubility because they strengthen solute:water intermolecular forces, even though this automatically [as implicit in the Barclay-Butler rule (132, 134) relating entropies of solution to heats of solution] reduces the system's degrees of freedom and causes a small loss of entropy. On the other hand, the effect of the $-CH_2-$ group in reducing water solubility and "pushing" the solute out of water proves to be entropy-controlled. For instance, comparison of $CH_3 \cdot CH_2OH$ and $CH_3 \cdot CH_2 \cdot CH_2OH$ yields $\delta\Delta F_w = +160$ cal/mole, $\delta\Delta H_w = -1540$ cal/mole, $\delta\Delta S_w = -5.7$ cal/mole/degree, $T\delta\Delta S_w = -1700$ cal/mole for the $-CH_2-$ group, which reduces solubility ($\delta\Delta F_w > 0$) because of an entropy effect ($\delta\Delta S_w < 0$) and despite the enthalpy term ($\delta\Delta H_w < 0$). Regarding the origin of $\delta\Delta F_l$'s in bulk lipid phases, thermal measurements of Butler & Harrower (135) prove that $\delta\Delta F_l$ for the $-CH_2-$ group in benzene is enthalpy-controlled, and the general validity of the Barclay–Butler rule in nonpolar solvents implies that $\delta\Delta F_l$'s for other groups are also enthalpy-controlled. $\delta\Delta F_{w\to l}$ for the $-CH_2-$ group and $\Delta F_{w\to l}$ for hydrocarbons and the higher alcohols prove to be entropy-controlled, $\Delta F_{w\to l}$ for the lower alcohols enthalpy-controlled, in the benzene:water system and presumably in other bulk lipid:water systems. The molecular interpretation of these large entropy effects associated with nonpolar residues in the aqueous phase is considered on p. 641.

Intermolecular forces.—The principal forces between nonelectrolytes and water depend upon hydrogen bonds, whereas the principal forces between nonelectrolytes and lipids are short-range van der Waals forces (forces between permanent dipoles, forces between a permanent dipole and an induced dipole, and London dispersion forces). The preceding thermodynamic analysis showed that selectivity in nonelectrolyte partition and permeation is dominated by interactions in the aqueous phase, and that these aqueous-phase interactions are enthalpy- rather than entropy-controlled except in the case of the $-CH_2-$ group. Thus, most of nonelectrolyte selectivity should be explicable in terms of hydrogen bonds. In fact, as recognized initially by Collander (95), the reduction in permeating power caused by a substituent can be predicted from the number and strength of hydrogen bonds it forms. As background to the following discussion it may be recalled that a hydrogen bond is a bridge formed by hydrogen between two electro-negative atoms acting as proton acceptor and proton donor, respectively; that the strongest bridges involve O as the donor and O or N as the acceptor (e.g., $CH_3–O–H\cdots NH(CH_3)_2$); and that dipole-dipole forces, resonance stabilization, and dispersion forces all contribute to the bridge strength. Spectroscopic studies (e.g., 136, 137) have shown that $-COOH > -CONH_2 >$ OH are the most effective donor groups, $-NH_2$ being considerably weaker; and that the approximate potency sequence for acceptors is

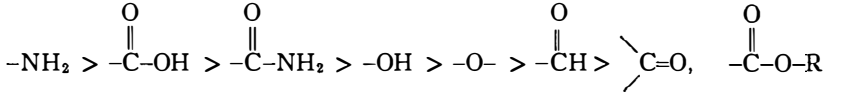

$> -C{\equiv}N > -NO_2$.

We shall consider in turn the primary hydrogen-bonding effects, secondary effects (intramolecular bonding and inductive effects), and the effect of the $-CH_2-$ group. More detailed discussion and examples will be found in the analysis by Diamond & Wright (99).

Primary effects.—

1. *Hydroxyl.* Of the six simple oxygen functions 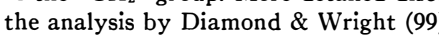 , the –OH group is the most potent 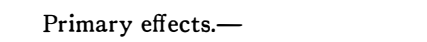 : it reduces P's in *Nitella mucronata* by 450 times, P's in *Chara ceratophylla* by 23 times, $K_{\text{isobutanol}}$ by 5 times, K_{ether} by 32 times, K_{oil} by 110 times, and is associated with the largest value of $\delta\Delta F_w$ after –COOH. This potency is due to the fact that –OH acts both as a proton donor () and as a proton acceptor (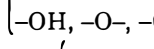), whereas –O–, 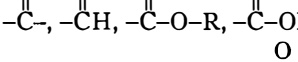 , and have no protons to donate and act only as acceptors. In addition, spectroscopic evidence shows that  –OH is a more effective acceptor than –O–, 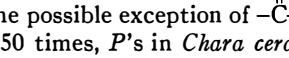 , or . Although an oxygen in a water molecule can accept two protons by using both of its unshared electron pairs, oxygen in most alcohols and other organic molecules can probably accept no more than one proton, so that the total number of H bonds formed by the alcoholic –OH group is estimated as two. Table I shows that –OH is relatively less potent ($-\delta\Delta F_w+\delta\Delta F_l$ is smaller) in reducing K_{ether} than K_{oil} or $P_{Nitella}$. This is because the –O– in ether acts as an acceptor for the hydroxyl proton, so that –OH shifts partition equilibrium by little more than one H bond in the ether:water system but by two bonds in the other systems.

2. *Ether.* The –O– link reduces K's and P's because it acts as a proton acceptor (but not donor). One's first expectation would be that, given a lipid phase devoid of H-bonding sites, two –O–'s should be as potent as one –OH in reducing K and P since –O– would form approximately one H bond, –OH two. Actually, the numerous comparisons provided by the gallbladder results (99, Table 3) show that two –O–'s are slightly less potent than one –OH. This is in agreement with the spectroscopic evidence that –O– is a somewhat less effective acceptor than –OH, presumably because of greater

steric hindrance to H bonding at the ether oxygen, which is flanked by two rather than one alkyl groups.

3, 4. *Aldehydes and ketones.* Earlier workers found that $-\overset{H}{\underset{|}{C}}=O$ and $\diagdown\!\!\diagup C=O$ were as potent as –OH in reducing P's, whereas one would have expected them to be only half as potent because they cannot act as proton donors. However, in aqueous solution many carbonyl compounds actually become rapidly transformed into hydroxy compounds, either through addition of water to the double bond $\left| \diagdown\!\!\diagup C=O \xrightarrow{H_2O} \diagdown\!\!\diagup \overset{OH}{\underset{OH}{C}} \right|$ or through intramolecular hydrogen migration forming an enolic tautomer $\left(-\overset{O}{\overset{\|}{C}}-CH_2 \rightarrow -\overset{OH}{\overset{|}{C}}=CH- \right)$. By repeated measurements of σ's beginning 1 min after first contact of aliphatic aldehydes with water, Wright & Diamond (97, Figure 4) showed that permeating power in the gallbladder decreased from an initially high value towards the value expected for a hydroxylated compound with a half-time of 150–300 sec, in agreement with rate constants for the aldehyde hydration reaction measured by purely physical techniques. Extrapolated zero-time σ's for aliphatic aldehydes, and σ's of two carbonyl compounds which are known neither to hydrate nor to enolize, show that the native carbonyl group does reduce permeability but by much less than the –OH group, as predicted from H-bond considerations (99).

5. *Esters.* The $-\overset{O}{\overset{\|}{C}}-OR$ group is less potent than –OH at reducing P's and K's, as expected from its possessing acceptor but not donor properties. Table I shows that its potency is of the same order as that of the ether oxygen, but the available evidence is inadequate to make a finer comparison between these two acceptor groups.

6. *Carboxyl.* Collander's evidence (95, Table 8) suggests that $-\overset{O}{\overset{\|}{C}}-OH$ and –OH have roughly comparable potencies in reducing K_{ether}, and this is also true for K_{oil} and $K_{isobutanol}$. Like –OH, –COOH is both a proton donor and a proton acceptor, and is more potent than oxygen functions lacking donor properties $\left(-O-, -\overset{O}{\overset{\|}{C}}-, -\overset{O}{\overset{\|}{C}}-H, -\overset{O}{\overset{\|}{C}}-OR \right)$ at reducing K_{oil} but only equally potent in its effect on K_{ether}, since ether itself is an acceptor.

7. *Amines.* $\left| -NH_2, \diagdown\!\!\diagup NH, -N\begin{matrix} R \\ \diagdown\!\!\diagup \\ R \end{matrix} \right|$. The amino group has nearly as high

a $\delta\Delta F_{to}$ as –OH, and is as potent or more so at depressing P's and K's. Primary amines ($-NH_2$) and secondary amines $\left(\diagdown\!\!\diagup NH\right)$ have both donor $\left(\diagdown\!\!\diagup N\text{–}H\cdots\cdots X\text{–}\right)$ and acceptor $\left(H\text{–}\underset{|}{N}\cdots\cdots H\text{–}X\text{–}\right)$ properties, while tertiary amines $\left(-N\begin{matrix}R\\ \diagdown\\ \diagup\\ R\end{matrix}\right)$ have only acceptor properties. However, inspection of Collander's K_{ether} and $K_{isobutanol}$ values shows that tertiary amino groups are somewhat more potent than secondary, and secondary more potent than primary, at depressing K's, which suggests that the effect of amino groups is mainly due to the acceptor properties of N's single unshared electron pair. This is in agreement with spectroscopic evidence that $-\diagdown\!\!\diagup N\cdots\cdots H\text{–}X\text{–}$ bridges are stronger than $\diagdown\!\!\diagup O\cdots\cdots H\text{–}X\text{–}$ bridges, because of greater resonance stabilization, but that $\diagdown\!\!\diagup N\text{–}H\cdots\cdots X\text{–}$ bridges are much weaker than either or than $-O\text{–}H\cdots\cdots X\text{–}$. The loss of the weak $\diagdown\!\!\diagup N\text{–}H\cdots\cdots X\text{–}$ bridges as one proceeds from $-NH_2$ to $\diagdown\!\!\diagup NH$ to $-\diagdown\!\!\diagup N$ is more than compensated by a strengthening of the $-\diagdown\!\!\diagup N\cdots\cdots H\text{–}X\text{–}$ bridge due to inductive effects of alkyl groups. In the ether: water system, where the acceptor properties of ether largely cancel effects of the solute's donor properties on partition and only the solute's acceptor properties are effective, amines are more potent than hydroxyls (Table I).

8. *Amides.* In the gallbladder, *Nitella*, isobutanol, and olive oil, the $-\overset{O}{\overset{\|}{C}}\text{–}NH_2$ group is more potent than one –OH but less potent than two –OH's in depressing P's and K's, while it is slightly more potent than two –OH's in its effect on K_{ether} (because –OH is less potent, not because $-\overset{O}{\overset{\|}{C}}\text{–}NH_2$ is more potent). This is as expected from the facts that $-\overset{O}{\overset{\|}{C}}\text{–}NH_2$ has two proton-ac-

cepting sites (O and N) as well as two protons to donate, and from the experimental finding (137) that $-\overset{\overset{O}{\|}}{C}-NH_2$ exceeds –OH both in acceptor and in donor abilities.

9. *Ureas.* In the gallbladder, *Nitella*, and olive oil derivatives of urea $\left(R-NH-\overset{\overset{O}{\|}}{C}-NH_2\right)$ have approximately the same K or P as dihydroxy alcohols with the same number of carbon atoms, because of the numerous proton donor and acceptor sites on the urea residue (nominally three each). As in the case of amines, the urea effect should be due mainly to its acceptor properties, and this is consistent with the fact that urea affects K_{oil} and K_{ether} equally, while –OH (for which donor and acceptor properties are equally important) affects K_{ether} less than K_{oil}.

10. *Nitriles.* In the gallbladder, $-C\equiv N$ reduces P by more than –O– but by less than –OH because of proton acceptance by the nitrogen and possibly by the π electrons of the triple bond as well. The difference between the permeabilities of aromatic compounds and homologous saturated compounds, and the complex effect of unsaturation in nonaromatic compounds $\left(\diagdown C=C\diagup \text{ and } -C\equiv C-\right)$, also arise in part from H bonding to π electrons (see 99 for details).

11. *Sulfur.* Sulfur compounds are more permeant and have higher K's than their oxygen analogues because of the much weaker H-bonding ability of sulfur. In the gallbladder and presumably in those other tissues where thiourea $\left(H_2N-\overset{\overset{S}{\|}}{C}-NH_2\right)$ is less permeant than urea $\left(H_2N-\overset{\overset{O}{\|}}{C}-NH_2\right)$, this arises from preferential permeation of urea via the polar route, not via lipid.

Secondary effects.—Stein (109), had the courage to try to predict permeability ratios for different nonelectrolytes by attributing a certain number of H bonds to each group regardless of its molecular environment and by counting up the number of each kind of group in a given molecule. His Figure 3.11 does succeed in predicting, within a factor of 5 for all solutes except water, the values of $PM^{1/2}$ which Collander (82) obtained for 48 nonelectrolytes in *Chara ceratophylla*. Since the P's spanned a range of 30,000, Stein's graph constitutes a good fit, which strikingly illustrates the controlling role and predictive power of H bonds in nonelectrolyte permeation.

The residual scatter in Stein's graph, and the scatter we encountered in experimental values of K ratios and P ratios for different pairs of compounds used to calculate the average $\delta\Delta F$ values in Table I, are due mainly to the fact that the molecular environment does affect somewhat the H-bonding

ability of a given group in two ways: intramolecular H bonding and inductive effects.

1. *Intramolecular H bonding.* If two groups on the same molecule, one a proton acceptor and the other a proton donor, are sufficiently close, an intramolecular H bond may be formed, reducing by up to two the number of H bonds that can be formed with water and therefore increasing P's or K's. A typical example is the decrease in gallbladder σ's (increase in permeability) among the isomeric dihydroxy cyclohexanes as the two –OH's are moved successively closer: 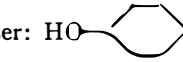 $\sigma = 1.02$, 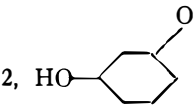 $\sigma = 0.94$, 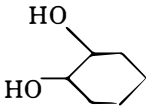 $\sigma = 0.54$. Evidently much of the latter molecule is in the form 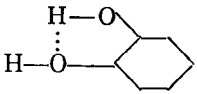 . Intramolecular H bonding must be considered in interpreting the permeation or distribution of almost any polyfunctional solute, and is the explanation of Overton's empirical rule that two substituents on a molecule are more potent the further apart they are. For the same reason, comparison of Butler's (131) ΔF_w's for hydrocarbons and their mono- and polyhydroxy derivatives yields smaller values of $\delta\Delta F_w$ for the –OH group when it is introduced next to another –OH group than when it is introduced into a pure hydrocarbon.

2. *Inductive effects.* As already mentioned in the discussion of ion permeation (p. 594), the electron density on a group (hence the group's proton-donating or -accepting ability) is modified by neighboring groups. Alkyl groups are electron-releasing, but most other groups, notably $-NO_2$ and halogens, are electron-withdrawing, this inductive effect decreasing with increasing distance between the modifying group and the affected group. Simple examples of inductive effects are provided by the gallbladder σ's of halogenated amides (99, Tables 8 and 9), which show that halogenation increases the permeating power of amides due to electron withdrawal from the amide N and O and hence reduction in proton-accepting abilities.

Hydrocarbon chain length and entropy effects.—The introduction of each $-CH_2-$ group into a molecule increases K_{oil}, K_{ether}, P in *Nitella*, and K's in many other lipid solvents by a factor of about 3, and increases narcotizing potency in tadpoles and other test objects by the same factor ("Ferguson's rule"). The thermodynamic analysis of pp. 630–35 showed that this is due partly to an enthalpy-dominated negative $\delta\Delta F_l$ "pulling" the solute into the lipid phase and readily attributable to increased van der Waals forces with lipids, but is also due to an entropy-dominated positive $\delta\Delta F_w$ which "pushes" the solute out of the aqueous phase and whose origin is less obvious. Diamond

& Wright (99) showed that the high partition coefficients of pure hydrocarbons, and, by implication, the high permeability coefficients of any solute with a large nonpolar residue, are primarily an entropy effect in the aqueous phase: i.e., $\Delta F_{w \to l}$ is dominated by the large negative value of the entropy of solution in water. Thus, as first recognized in a classic study by Frank & Evans (132), hydrocarbons and hydrocarbon residues, because of their weak force fields, behave in aqueous solution as if they permitted increased ordering of surrounding water molecules and stabilized adjacent H-bonded water clusters, a phenomenon which Frank & Evans pictorially described as "icebergs". Solutes with long hydrocarbon chains are driven into the lipid phase by the gain in entropy resulting from "melting" of the "iceberg" [see (99, 132, 133, 138, 139) for further discussion of these entropy effects]. Similarly, halogens exercise a direct effect in increasing K's and P's analogous to that of $-CH_2-$ and distinct from their inductive effects (99). Calculation of K's for chloroform ($CHCl_3$), which is highly permeant in the gallbladder, from the thermal data of Frank & Evans (132) shows that this direct effect of halogens is also an entropy effect in the aqueous phase.

Controlling Variables in Main-Pattern Selectivity

The most conspicuous differences between the nonelectrolyte permeability patterns of different cells concern small polar solutes and are apparently due to differences in the importance of the polar route. Otherwise the selectivity patterns of all cells are quite similar. What differences do exist between main-pattern selectivities (i.e., selectivities associated with permeation via membrane lipids) appear to be of two sorts:

1. *Selectivity magnitudes.* Although main-pattern selectivity sequences differ little from cell to cell, there are significant quantitative differences in the ranges of selectivity. For instance, comparison of three related algae shows that "in *Nitella* the permeability to methanol is 180,000 times, in *Nitellopsis* 21,000 times, and in *Chara* only 2600 times greater than that of glycerol" (81, p. 443). P's are proportional to $(K_{oil})^{1.32}$ in *Nitella*, to $(K_{oil})^{1.15}$ in *Nitellopsis*, and to $(K_{oil})^{1.0}$ in *Chara*. The $-OH$ group reduces P's on the average by 450 times in *Nitella*, by only 23 times in *Chara*.

Collander's studies (92–96) on K's of bulk lipid solvents suggest that the molecular parameter governing these quantitative differences is the ratio of hydrogen-bonding groups to $-CH_2-$ groups in the membrane interior: the lower this ratio, the lower are the values of ΔF_l, the larger is $(-\Delta F_w + \Delta F_l)$, and hence the higher are the magnitudes of selectivity. The reason is that hydrogen-bond energies are considerably stronger than van der Waals attractions to hydrocarbons, so that solvent hydrogen-bonding groups in a predominantly lipid phase markedly increase solute:lipid forces and ΔF_l's. For instance, analysis of Collander's studies of monohydroxy alcohols of varying chain length as solvents shows that the $-OH$ group decreases K's on the average by 5.2 times in C_4H_9OH, by 7.2 times in $C_5H_{11}OH$, by 8.5 times in $C_8H_{17}OH$, by 14.7 times in $C_{15}H_{35}OH$, by 107 times in olive oil, by

1300 times in benzene, and P's by 450 times in *Nitella*. From these values one can calculate that the incremental free energy of solution $\delta\Delta F$ associated with the –OH group decreases from -6970 cal/mole in water, to -6000 cal/mole in C_4H_9OH (isobutanol), to -5400 cal/mole in $C_{18}H_{35}OH$, to -3300 cal/mole in *Nitella*, to -2700 cal/mole in benzene. K's measured separately between two different lipid solvents a or b and water are related by an equation of the form $K_a = x(K_b)^y$ in which, for a given solvent b, the exponent y, which measures the magnitude of selectivity, increases with increasing chain length of solvent a if a is an aliphatic alcohol. As another example, Table I shows that isobutanol, which has a higher ratio of H-bonding sites to $-CH_2-$ groups than does ether or olive oil, has the highest values of $\delta\Delta F_l$ (nearly comparable to $\delta\Delta F_w$, the values in water) and the lowest range of selectivity ($-\delta\Delta F_w + \delta\Delta F_l$) of the lipid solvents studied. Thus, a very few hydrogen-bonding groups in the membrane interior, by increasing lipid:solute forces from the low values typical of a pure hydrocarbon towards the high values prevailing in water, could markedly depress selectivity ratios. The facts that *Nitella* P's are proportional to $(K_{oil})^{1.32}$, and that the –OH group depresses *Nitella* P's by a larger factor than K's for olive oil or $C_{18}H_{35}OH$, suggest that the interior of a *Nitella* cell membrane is much closer to a pure hydrocarbon than even an 18-carbon monohydroxy alcohol. The same conclusion follows from the fact that one –OH group offsets the change in P or σ produced by six $-CH_2-$ groups in *Nitella* or the gallbladder (99), but offsets the effect of only 5.3 $-CH_2-$ groups on K's in benzene, 4.3 in olive oil, 2.15 in $C_{18}H_{35}OH$, and 1.86 in C_4H_9OH.

2. *Membrane "acidity"*. The extensive botanical literature on permeability shows that some cells, while normal in other respects, are unusually permeable to basic solutes like amides (88). This has been interpreted to mean that such cells have unusually "acidic" cell membranes, by analogy with the fact that addition of small quantities of acids to an organic phase increases K's for bases in that phase. Expressed in more general terms, a few proton-donor groups in the membrane might selectively improve permeability to proton acceptors due to H-bond formation (hence higher ΔF_l's) in the membrane. An illustration of the opposite effect (preferential permeability to proton donors) is that the –OH and –COOH groups are less effective at reducing K's in ether than in olive oil (Table I), so that a membrane composed of an ether phase would be more permeable to alcohols and acids. Ether and olive oil are otherwise similar in their solubility properties, but the –O– of ether is a proton acceptor, increasing $\delta\Delta F_l$'s and K's for proton-donating solutes.

Summary of Nonelectrolyte Selectivity

For the overwhelming majority of nonelectrolytes the selectivity patterns of biological membranes are very similar to the selectivity patterns of a bulk lipid phase, so that the explanation for nonelectrolyte selectivity must be sought largely in the differences between solute:water and solute:lipid

intermolecular forces. Exceptions to this main pattern are that branched molecules are less permeant, and the inverse relation between permeating power and molecular size is apparently steeper, than that found for permeation through a bulk lipid phase; these differences are attributed to the more organized structure of lipids in cell membranes. In addition, small polar solutes permeate more rapidly than they would through a bulk lipid phase; the interpretation supported by several lines of evidence is that some predominantly polar regions in the membrane provide a parallel permeation pathway that bypasses membrane lipids. Analysis of incremental free energies of solution in water, bulk lipids, or membranes, associated with specific functional groups, shows that the main pattern of selectivity is largely due to differences in water:solute intermolecular forces: the stronger these forces, the lower the solute's permeating power. The most important contributing forces are hydrogen bonds, modification of hydrogen bonding by inductive effects and intramolecular bonds, van der Waals forces in membrane lipids, and entropy effects in hydrocarbon:water interactions. Main-pattern permeability differences between different biological membranes are principally determined by the ratio of hydrogen-bonding groups to $-CH_2-$ groups in the membrane interior, and by whether these hydrogen-bonding groups are proton donors or proton acceptors.

ACKNOWLEDGMENTS

It is a pleasure to record our debt to Dr. George Eisenman for valuable and generous advice on ion selectivity and for his criticism of the first half of this chapter; to Drs. P. H. Barry, R. S. Eisenberg, and A. D. Grinnell for critical readings of the manuscript; and to Dr. H. S. Sherry for discussion of divalent cation selectivity.

LITERATURE CITED

1. Eisenman, G. *Biophys. J.*, **2**, Part 2, 259–323 (1962)
2. Eisenman, G. In *Symposium on Membrane Transport and Metabolism*, 163–79 (Kleinzeller, A., Kotyk, A., Eds., Academic Press, New York, 608 pp., 1961)
3. Eisenman, G. *Proc. 23rd Intern. Congr. Physiol. Sci., Tokyo*, 489–506 (Excerpta Med. Found., Amsterdam, 644 pp., 1965)
4. Reichenberg, D. In *Ion Exchange*, **I** 227–76 (Dekker, New York, 424 pp., 1966)
5. Sherry, H. S. In *Ion Exchange*, **II** (Dekker, New York, in press, 1968)
6. Truesdell, A. H., Christ, C. L. In *Glass Electrodes for Hydrogen and Other Cations*, 293–321 (Dekker, New York, 582 pp., 1967)
7. Jaeger, F. M. *Trans. Faraday Soc.*, **25**, 320–45 (1929)
8. Pauling, L. *The Nature of the Chemical Bond* (Cornell Univ. Press, Ithaca, N. Y., 450 pp., 2nd ed., 1948)
9. Jenny, H. *J. Phys. Chem.*, **36**, 2217–58 (1932)
10. Barrer, R. M., Rees, L. V. C., Ward, D. J. *Proc. Roy. Soc. A*, **273**, 180–97 (1963)
11. Hughes, W. S. *J. Am. Chem. Soc.*, **44**, 2860–67 (1922)
12. Eisenman, G., Rudin, D. O., Casby, J. U. *Science*, **126**, 831–34 (1957)
13. Eisenman, G. *Advan. Anal. Chem. Instr.*, **4**, 213–369 (1965)
14. Eisenman, G. *Bol. Inst. Estud. Méd. Biol.* **21**, 155–83 (1963)
15. Berridge, M. J. *J. Exptl. Biol.*, **48**, 159–74 (1968)
16. Wright, E. M., Diamond, J. M. *Biochim. Biophys. Acta*, **163**, 57–74 (1968)
17. Chandler, W. K., Meves, H. *J. Phys-*

iol. (*London*), **180**, 788–820 (1965)
18. Gillary, H. L. *J. Gen. Physiol.*, **50**, 359–68 (1966)
19. Pressman, B. C. *Ann. N.Y. Acad. Sci.* (In press) (1968)
20. Mueller, P., Rudin, D. O. *Biochem. Biophys. Res. Commun.*, **26**, 398–404 (1967)
21. Lev, A. A., Buzhinsky, E. P. *Tsitologiia*, **9**, 102–6 (1967)
22. Andreoli, T. E., Tieffenberg, M., Tosteson, D. C. *J. Gen. Physiol.*, **50**, 2527–34 (1967)
23. Eisenman, G., Ciani, S., Szabo, G. *Fed. Proc.* (In press) (1968)
24. Pedersen, C. J. *J. Am. Chem. Soc.*, **89**, 7017–36 (1967)
25. Pedersen, C. J. *Fed. Proc.* (In press) (1968)
26. Lindeman, B. *Exptl. Eye Res.*, **7**, 62–69 (1968)
27. Forte, J. G., Forte, G. M., Saltman, P. *J. Cell Physiol.*, **69**, 293–304 (1967)
28. Bungenberg de Jong, H. G. In *Colloid Science*, **II**, 259–334 (Kruyt, H. R., Ed., Elsevier, New York, 753 pp., 1949)
29. Barber, R., Noble, M. *Biochim. Biophys. Acta*, **123**, 205–206 (1966)
30. Armstrong, W. McD., Rothstein, A. *J. Gen. Physiol.*, **50**, 967–88 (1967)
31. Ling, G. N., Ochsenfeld, M. M. *J. Gen. Physiol.*, **49**, 819–43 (1966)
32. Warren, J. C., Stowring, L., Morales, M. F. *J. Biol. Chem.*, **241**, 309–16 (1966)
33. Sjodin, R. A., Beaugé, L. A. *J. Gen. Physiol.* **51**, No. 5, Part 2, 152s–161s (1968)
34. Baker, P. F., Connelly, C. M. *J. Physiol.* (*London*), **185**, 270–97 (1966)
35. Lindley, B. D., Hoshiko, T. *J. Gen. Physiol.*, **47**, 749–71 (1964)
36. Maizels, M. *J. Physiol.* (*London*), **195**, 657–79 (1968)
37. Katz, A. M. *Biochim. Biophys. Acta*, **162**, 79–85 (1968)
38. Kuznetsov, I. A., Mezentsev, A. N., Moshkovskii, Y. S., Lukanin, A. S. *Biophysics*, **12**, 425–30 (1967)
39. Wiegner, G., Jenny, H. *Kolloid Z.*, **42**, 268–74 (1927)
40. Teunissen, P. H., Bungenberg de Jong, H. G. *Kolloid-Beiheft*, **48**, 33–57 (1939)
41. Gregor, H. P., Bregman, J. I. *J. Colloid Sci.*, **6**, 323–47 (1951)
42. Ling, G. N. In *Phosphorus Metabolism*, **II**, 748–97 (McElroy, W. D., Glass, B., Eds., Johns Hopkins Press, Baltimore, 930 pp., 1952)
43. Ling, G. N. *A physical theory of the living state: the association-induction hypothesis* (Blaisdell, New York, 680 pp., 1962)
44. Diamond, J. M., Wright, E. M. *Fed. Proc.*, **27**, 748 (1968)
45. Teunissen, P. H. Rosenthal, S., Zaaijer, W. H. *Rec. Trav. Chim. Pays Bas*, **57**, 929–40 (1938)
46. Rossini, F. D., Wagman, D. D., Evans W. H., Levine, S., Jaffe, I. *Selected Values of Chemical Thermodynamic Properties* (U.S. Govt. Printing Office, Washington, 1952)
47. Rosseinsky, D. R. *Chem. Rev.*, **65**, 467–90 (1965)
48. Bregman, J. I. *Ann. N.Y. Acad. Sci.*, **57**, 125–43 (1953)
49. Castillo, J. del, Mello, W. C. de, Morales, T. *J. Gen. Physiol.*, **48**, 129–40 (1964)
50. Takagi, S. F., Wyse, G. A., Yajima, T. *J. Gen. Physiol.*, **50**, 473–89 (1966)
51. Takeuchi, A., Takeuchi, N. *J. Physiol.* (*London*), **191**, 575–90 (1967)
52. Tosteson, D. C. *Acta Physiol. Scand.*, **46**, 19–41 (1959)
53. Araki, T., Ito, M., Oscarsson, O. *J. Physiol.* (*London*), **159**, 410–35 (1961)
54. Hutter, O. F., Hoble, D. *J. Physiol.* (*London*), **157**, 335–50 (1961)
55. Hutter, O. F., Padsha, S. M. *J. Physiol.* (*London*), **146**, 117–32 (1959)
56. Finkelstein, A., Cass, A. *J. Gen. Physiol.*, **52**, No. 5, Part 2, 145s–172s (1968)
57. Tasaki, I., Singer, I., Takenaka, T. *J. Gen. Physiol.*, **48**, 1095–1123 (1965)
58. Jhamandas, K. H., Nash, C. W. *Can. J. Physiol. Biochem.*, **45**, 675–82 (1967)
59. Lindskog, S. *Biochemistry*, **5**, 2641–46 (1966)
60. Truesdell, A. H. *Study of natural glasses through their behavior as membrane electrodes* (Ph.D. thesis, Harvard Univ., Cambridge, Mass., 1962)
61. Ames, L. L. *Am. Mineralogist*, **49**, 1099–1110 (1964)
62. Bangham, A. D., Pethica, B. A., Seaman, G. V. F. *Biochem. J.*, **69**, 12–19 (1958)
63. Goldner, A. M., Cassidy, M. M., Tidball, C. S. *Proc. Soc. Exptl. Biol. Med.*, **124**, 884–87 (1967)
64. Hagiwara, S., Takahashi, K. *J. Gen. Physiol.*, **50**, 583–601 (1967)

65. Findlay, G. P., Hope, A. B. *Australian J. Biol. Sci.*, **17**, 400–11 (1964)
66. Toda, H., Narita, K. *J. Biochem.*, **62**, 767–68 (1967)
67. Ponder, E. *J. Gen. Physiol.*, **36**, 767–75 (1953)
68. Kasai, M., Oosawa, F. *Biochim. Biophys. Acta*, **154**, 520–28 (1968)
69. Weinstock, A., King, P. C., Wuthier, R. E. *Biochem. J.*, **102**, 983–88 (1967)
70. Blaustein, M. P., Goldman, D. E. *J. Gen. Physiol.*, **51**, No. 5, Part 2, 279–91 (1968)
71. Koefoed-Johnsen, V., Ussing, H. H. *Acta Physiol. Scand.*, **42**, 298–308 (1958)
72. Moeller, T. *Inorganic Chemistry* (Wiley, New York, 966 pp., 1957)
73. Eisenman, G. *Neurosciences Research* (In preparation)
74. Mullins L. J. In *Molecular Structure and Functional Activity of Nerve Cells*, 123–66 (Grenell, R. G., Mullins, L. J., Eds., AIBS, Washington, 169 pp., 1956)
75. Lindley, B. D. *J. Theoret. Biol.*, **17**, 213–28 (1967)
76. Robinson, R. A., Stokes, R. H. *Electrolyte Solutions* (Butterworths, London, 2nd ed. revised, 571 pp., 1965)
77. Solomon, A. K. *J. Gen. Physiol.*, **51**, No. 5, Part 2, 335s–364s (1968)
78. Tosteson, D. C., Cook, P., Andreoli, T., Tieffenberg, M. *J. Gen. Physiol.*, **50**, 2513–25 (1967)
79. Lardy, H. A., Graven, S. N., Estrada-O., S. *Fed. Proc.*, **26**, 1355–60 (1967)
80. Glueckauf, E. *Proc. Roy. Soc. A*, **214**, 207–25 (1952)
81. Collander, R. *Physiol. Plantarum*, **7**, 420–45 (1954)
82. Collander, R., Bärlund, H. *Acta Botan. Fennica*, **11**, 1–114 (1933)
83. Collander, R. *Physiol. Plantarum*, **3**, 45–57 (1950)
84. Collander, R. *Ibid.*, **2**, 300–11 (1949)
85. Collander, R., Wikström, B. *Physiol. Plantarum*, **2**, 235–46 (1949)
86. Collander, R. *Physiol. Plantarum*, **12**, 139–44 (1959)
87. Collander, R. *Ibid.*, **13**, 179–85 (1960)
88. Collander, R. *Trans. Faraday Soc.*, **33**, 985–90 (1937)
89. Collander, R. *Protoplasma*, **46**, 123–42 (1956)
90. Collander, R. *Physiol. Plantarum*, **10**, 397–405 (1957)
91. Oura, E., Suomalainen, H., Collander, R. *Physiol. Plantarum*, **12**, 534–44 (1959)
92. Collander, R. *Acta Physiol. Scand.*, **13**, 363–81 (1947)
93. Collander, R. *Acta Chem. Scand.*, **4**, 1085–98 (1950)
94. Collander, R. *Ibid.*, **5**, 774–80 (1951)
95. Collander, R. *Ibid.*, **3**, 717–47 (1949)
96. Wartiovaara, V., Collander, R. *Protoplasmatologia*, **2C8d**, 1–98 (1960)
97. Wright, E. M., Diamond, J. M. *Proc. Roy. Soc. B* (In press) (1968)
98. Wright, E. M., Diamond, J. M. *Ibid.*
99. Diamond, J. M., Wright, E. M. *Ibid.*
100. Kedem, O., Katchalsky, A. *Biochim. Biophys. Acta*, **27**, 229–46 (1958)
101. Dainty, J., Ginzburg, B. *Z. J. Theoret. Biol.*, **5**, 256–65 (1963)
102. Smyth, D. H., Wright, E. M. *J. Physiol. (London)*, **182**, 591–602 (1966)
103. Diamond, J. M., Harrison, S. C. *J. Physiol. (London)*, **183**, 37–57 (1966)
104. Dainty, J. *Advan. Botan. Res.*, **1**, 279–326 (1963)
105. Dainty, J., House, C. R., *J. Physiol. (London)*, **185**, 172–84 (1966)
106. Dainty, J., Ginzburg, B. *Z. Biochim. Biophys. Acta*, **79**, 122–28 (1964)
107. Overton, E. *Vjschr. Naturforsch. Ges. Zürich*, **44**, 88–135 (1899)
108. Spandau, H. *Ber. Deut. Chem. Ges.*, **74**, 1028–30 (1941)
109. Stein, W. D. *The Movement of Molecules across Cell Membranes* (Academic Press, New York, 369 pp., 1967)
110. Davson, H., Danielli, J. F. *The Permeability of Natural Membranes* (Cambridge Univ. Press, Cambridge, 365 pp., 1952)
111. Zwolinski, B. J., Eyring, H., Reese, C. E. *J. Phys. Colloid Chem.*, **53**, 1426–53 (1949).
112. Wartiovaara, V. *Physiol. Plantarum*, **3**, 462–78 (1950)
113. Tedeschi, H., Harris, D. L. *Arch. Biochem. Biophys.*, **58**, 52–67 (1955)
114. Rosen, H., Leaf, A., Schwartz, W. B. *J. Gen. Physiol.*, **48**, 379–89 (1964)
115. Wartiovaara, V. *Ann. Botan. Soc. Zool. Botan. Fennicae Vanamo*, **16**, 1–111 (1942)
116. Wartiovaara, V. *Physiol. Plantarum*, **2**, 184–96 (1949)
117. Wartiovaara, V. In *Handbuch der Pflanzenphysiologie*, **2**, 369–80 (Ruhland, W., Ed., Springer, Berlin, 1072 pp., 1956)
118. Jacobs, M. H., Glassman, H. N., Parpart, A. K. *J. Cellular Comp. Physiol.*, **7**, 197–225 (1935)
119. Höber, R., Ørskov, S. L. *Pflügers Arch.*, **231**, 599–615 (1933)

120. Vargas, F. *J. Gen. Physiol.*, **51**, No. 5, Part 2, 123s–130s (1968)
121. Villegas, R., Bruzual, I. B., Villegas, G. M. *J. Gen. Physiol.*, **51**, No. 5, Part 2, 81s–92s (1968)
122. Ruhland, W., Hoffmann, C. *Planta*, **1**, 1–83 (1925)
123. Schönfelder, S. *Planta*, **12**, 414–504 (1930)
124. Gutknecht, J. *Biochim. Biophys. Acta*, **163**, 20–29 (1968)
125. Kavanau, J. L. *Structure and Function in Biological Membranes*, **1** (Holden-Day, San Francisco, **321** pp., 1965)
126. Sha'afi, R. I., Rich, G. T., Sidel, V. W., Bossert, W. H., Solomon, A. K. *J. Gen. Physiol.*, **50**, 1377–99 (1967)
127. Andersen, B., Ussing, H. H. *Acta Physiol. Scand.*, **28**, 60–76 (1953)
128. Barry, P. H., Hope, A. B. *Biophys. J.* (In press) (1969)
129. Rich, G. T., Sha'afi, R. I., Barton, T. C. Solomon, A. K. *J. Gen. Physiol.*, **50**, 2391–2405 (1967)
130. Dainty, J., Ginzburg, B. *Z. Biochim. Biophys. Acta*, **79**, 129–37 (1964)
131. Butler, J. A. V. *Trans. Faraday Soc.*, **33**, 229–36 (1937)
132. Frank, H. S., Evans, M. W. *J. Chem. Phys.*, **13**, 507–32 (1945)
133. Franks, F. *Ann N.Y. Acad. Sci.*, **125**, 277–89 (1965)
134. Barclay, I. M., Butler, J. A. V. *Trans. Faraday Soc.*, **34**, 1445–54 (1938)
135. Butler, J. A. V., Harrower, P. *Trans. Faraday Soc.*, **33**, 171–78 (1937)
136. Gordy, W., Stanford, X. C. *J. Chem. Phys.*, **8**, 170–77 (1940)
137. Mizushima, S. *Structure of Molecules and Internal Rotation* (Academic Press, New York, 244 pp., 1954)
138. Aranow, R. H., Witten, L. *J. Phys. Chem.*, **64**, 1643–48 (1960)
139. Miller, K. W., Hildebrand, J. H. *J. Am. Chem. Soc.*, **90**, 3001–4 (1968)